RESEARCH ARTICLE

In silico assessment of the binding of reported bioactive compounds from *Phaseolus vulgaris* L. (Fabaceae) towards the wild-type and mutant estrogen receptor-alpha

Robertson G. Rivera^{1*}, Joanna V. Toralba¹, Junie B. Billones²

ABSTRACT

Background: Breast cancer is one of the leading causes of deaths in women worldwide, affecting nearly 7.8 million people. In 2020 in the Philippines, there were around 150,000 Filipinos who were newly diagnosed with the disease. The complex pathogenesis of breast cancer in addition to the emergence of resistance to therapy makes the treatment very challenging. Compounds that can antagonize the effects of estradiol towards $ER-\alpha$, especially the mutant Y537S type are sought for.

Objectives: The focus of this study was the *in-silico* assessment of the reported secondary metabolites from *Phaseolus vulgaris* L. (fam. Fabaceae) towards the wild-type and mutant ER- α . Bioisosteric replacement was conducted to generate analogs that can possibly have a comparable binding affinity as estradiol towards estrogen receptors alpha.

Results: Majority of the secondary metabolites present in *Phaseolus vulgaris* L. belong to the group of phytoestrogens, phytosterols, and plant hormones. These groups of compounds exhibited favorable binding energies toward the wild-type and mutant (Y537S) estrogen receptors alpha. Moreover, they bind to the same ligand binding pocket as estradiol, involving similar interactions and amino acid residues.

Conclusion: Compounds from *Phaseolus vulgaris* L. can potentially target ER- α . Four gibberellin A19 analogs were generated that exhibited favorable binding towards the wild- and mutant- ER- α and may be further optimized to obtain a promisin geompound against breast cancer.

Keywords: breast cancer, $ER-\alpha$, Phaseolus vulgaris L., in silico screening, molecular docking, Baguio beans

Introduction

Breast cancer is a collection of malignancies which affect the mammary gland and may metastasize to other parts of the body. It is a multifactorial disease involving estrogen, estrogen receptors, and inflammatory response, among others. It affects nearly 2.1 million women yearly and accounts for about 600,000 deaths in 2018 [1,2]. From 2015 to 2020, 7.8 million women were diagnosed with the disease, making it the most prevalent type of cancer worldwide [3]. In the Philippines, breast cancer is the most common type of cancer, leading to more than 200,000 new cases in both sexes and an estimated 7000 deaths [4]. It has affected around 350,000 Filipinos (male and female) in the last five years. In the year 2020, there are around 150,000 Filipinos who were newly diagnosed with the disease [2].

Several risk factors such as being female, age of menopause, genetic predisposition involving BRCA1 and BRCA2, early menarche, and high levels of endogenous sex hormones are attributed to the development of breast cancer [5-7].

About 70% of breast cancer patients test positive for ER- α , the receptor which is responsible for enhanced cellular proliferation the activation of which contributes to the pathogenesis of the disease [8]. ER- α is a transcription factor encoded by the ESR1 gene located at chromosome number 6. Mutations in the ESR1 gene are observed in metastatic breast cancers that are previously treated with aromatase inhibitors and are associated with a recalcitrant disease and worse prognosis. The most common site of mutation is in

^{*}Corresponding author's email address: rdrivera5@up.edu.ph

¹Department of Pharmaceutical Chemistry, College of Pharmacy, University of the Philippines Manila, Manila, Philippines

²Department of Physical Sciences and Mathematics, College of Arts and Sciences, University of the Philippines Manila, Manila, Philippines



the ligand binding domain at Y537 (tyrosine-537 residue) and D538 (aspartic acid-538 residue). These mutations result in a constitutively active receptor, independent of estrogen [10]. The Y537S (tyrosine 537 residue replaced with serine) and the D538G (aspartic acid replaced with glycine) mutations are prevalent and results in a reduced affinity of both tamoxifen and estrogen on the mutant receptors [8,10,15,16]. Other mutations may lead to estrogen hypersensitivity (K303R—lysine 303 replaced with arginine; E380Q—glutamate 380 replaced with glutamine) or a retained estrogen-dependent activity (S432L—serine 432 replaced with lysine; V534E—valine 534 replaced with glutamate) [10]. Among the mutations, the Y537S isoform is the most aggressive type with a 20-month survival rate [25].

While the pathophysiology of breast cancer is complex, Joshi and Press (2018) summarized the hallmarks of cancer which include sustained proliferative signaling, evasion of growth suppressors, resistance to cell death, induction of angiogenesis, activation of invasion and metastasis, evasion of immune destruction, reprogramming of bioenergetics, tumor-promoting inflammation, and genome instability and mutation which enables replicative immortality [13]. These hallmarks have been targets of breast cancer research and the identified biomarkers such as the estrogen receptors, progesterone receptors, and human epidermal growth factor (HER2) are keys in the current therapy [9].

Several treatment options for breast cancer are available depending on the presence or absence of markers such as ER- α and HER-2. These include the anti-estrogenic drug tamoxifen, anti-aromatase drugs such as exemestane and letrozole;, and other chemotherapy drugs like taxanes and doxorubicin, and the anti-HER2 drugs trastuzumab and pertuzumab [6]. However, development of resistance is possible [14] and toxicities such as asthenia, myelosuppression, and disruption of sensory signals are observed with the current treatments [6]. Mutations in the ESR1 gene which codes for the ER- α acquired from previous treatments with aromatase inhibitors is are one of the mechanisms by which resistance and a recalcitrant disease develops. Hence, one of the strategies against breast cancer is to target the mutant $ER-\alpha$. Moreover, adjunct treatments or key treatments with few to no side effects are continuously sought for [8,10,15,16].

Several studies have shown the potential of *Phaseolus vulgaris* L. (PVL) against cancer based on the dose-activity relationships [17-21]. *Phaseolus vulgaris* L. belongs to the family of legumes and is very common in the Philippines. The bean is a good source of protein, nutrients, and phytochemicals. Abu-

Reidah, et al. (2012) reported that most of the phenolics found in the bean are flavonoids and flavonoid derivatives [22]. These flavonoids belong to the phytoestrogens group of compounds which are nonsteroidal secondary metabolites having structural similarity and hence bioactivity as that of endogenous estrogens. Because of their ability to interact with the estrogen receptors, they can elicit estrogenic and antiestrogenic effects. These include modulation of bone homeostasis, cardiovascular effects, and reproductive effects [23]. Additionally, the beans contain phaseolin and lectin which are proteins that exhibit biological activities such as agglutination, mitosis, and cell growth inhibition [20].

The numerous bioactivities of the compounds from *Phaseolus vulgaris* L. make it a promising natural product against breast cancer. This study focused on *in silico* screening of the secondary metabolites from *Phaseolus vulgaris* L. against the wild-type and mutant $ER-\alpha$. Bioisosteric replacement in the structure of hit compounds was utilized as a strategy to determine analogs that may possibly have a better binding energy than the parent compounds. The present study may provide insights on how the bioactive compounds of *Phaseolus vulgaris* L. (Fabaceae) bind to $ER-\alpha$, especially the mutant receptors.

Methodology

Literature Search of Compounds from Phaseolus vulgaris L. (PVL) and Initial Screening

Literature search was conducted to identify the compounds that are present in PVL. Research articles which included methods of identification of PVL compounds were used. Only the secondary metabolites were included. For the glycosides, only the aglycone portion was considered for screening since glycosides are too polar to be absorbed via passive diffusion, hence, only the aglycones are likely to be absorbed. Moreover, in the screening process, they either fail the topological polar surface area (a parameter of oral bioavailability) or the drug-likeness filters. ADMETIab 2.0 (open source at https://admetmesh.scbdd.com/) was used for the primary screening of compounds [24]. In this study, the SMILES strings were obtained from the PubChem database. Both the canonical SMILES and the isomeric SMILES were used in the web server. The compounds considered for further evaluation were nonmutagenic/noncarcinogenic, have good oral bioavailability or high intestinal absorption, and have passed any of the drug-likeness rules (Lipinski rule, quantitative estimate of drug-likeness).



Protein and Ligand Structure

Thirteen ER- α receptor crystal structures were used in this study. These include one wild-type (PDB ID: 1A52) and twelve mutagenic Y537S receptor models (PDB ID: 3UUD, 4ZNS, 4ZNV, 5DXE, 5DXG, 5KCD, 5KCT, 5KD9, 5TLT, 5TM8, 5TN4, and 5TN5). The crystal structures of the receptors with their corresponding co-crystallized ligands are available at the protein data bank website (https://www.rcsb.org/). The Y537S mutation was chosen because it is one of the most common ER- α mutations and is the most aggressive [25]. All the mutant crystal structures have a resolution of 1.5 Å -2 Å whereas the wild-type has a 2.8 Å resolution. These crystal structures were also utilized by Shylaja *et al.* [26].

The 3-D structures of the ligands were downloaded from PubChem (https://pubchem.ncbi.nlm.nih.gov/) as SDF file format [27]. For ligands with isomeric SMILES, these were copied and pasted into the Swiss ADME web server to generate the 2-D structures. The 2-D structures generated were then processed using ChemSketch 2021.1.1 (https://www.acdlabs.com/resources/free-chemistry-software-apps/chemsketch-freeware/) to generate the 3-D structures [29]. These were saved as MOL files. All ligands were converted to PDB files before ligand processing and molecular docking.

Preparation of Protein

All protein crystal structures were downloaded from the protein data bank (www.rcsb.org) as PDB file. The proteins were processed using AutoDockTools v1.5.6 using the standard protocol [30]. Briefly, the file was opened using Autodock tools (ADT) and then water molecules were deleted, nonpolar hydrogens were merged, polar hydrogens were added, co-crystallized ligands, and other molecules not part of the receptor were deleted. Missing residues were repaired and Kollmann charges were then added.

Preparation of PVL Ligands

The ligands files in the SDF and MOL file formats were converted into PDB file format using Open Babel v3.1.1 [31]. The PDB files were then processed using ADT to add charges, merge nonpolar hydrogens, and add polar hydrogens. The final structures of the ligands were checked to ensure that the correct structures were generated because it was observed during the initial preparation steps that the ADT has the tendency to detect closely spaced atoms as bonded atoms. The outputs were in PDBQT file format.

Gridbox Optimization

To obtain the coordinates of the gridbox (search space) that were used in the molecular docking simulation, the proteins (PDB file format) were opened using Discovery Studio Visualizer v21.1.0.20298. In the graphic-user interface, the Receptor-Ligand Interactions tab was clicked, and, in this panel, the receptor was defined, and the site was defined based on PDB records. The active site will appear in the right-hand panel as a sphere. The sphere was clicked, and the attributes were determined. Here, the coordinates of the active site will appear as XYZ coordinates. These coordinates are used in the ADT and the search space was adjusted such that the volume did not exceed 27,000 Å3. Moreover, the ligand binding site was contained within the search space. The final volume used in the search space was 22 x 22 x 22 Å 3.

The ligands co-crystallized with the receptors were redocked in the receptor using Autodock Tools v1.5.6 and Autodock Vina v1.1.2. The number of modes was set to 10, the energy range was set to 3, and exhaustiveness was set to 8. It was ensured that the RMSD values with respect to the original pose of the crystallized ligand were less than 2 Å [32]. The grid box validation parameters and results are shown in Supplementary Table 1 and Supplementary Figure 1.

Molecular Docking

All molecular docking simulations were performed using Autodock Vina [32]. The standard protocol of for running Autodock Vina provided by Forli et al. (2016) was utilized [30]. The binding affinity (kcal/mol) of each ligand and receptor pair was calculated. The binding affinities of the native ligand estradiol (E2), and the selective estrogen receptor modulator, tamoxifen, were used as the reference values. PVL ligands with binding affinity values that are +2.5 kcal/mol with respect to these reference values were considered in the analyses. This threshold is a conservative estimate of the standard error (2.8 kcal/mol) of the results obtained from Autodock Vina [32]. Also, the binding affinities of the PVL ligands with respect to the 13 receptor models were considered. That is, they have negative binding affinity values across the receptor models and were within the +2.5 kcal/mol binding energy with respect to the reference compounds. Ligands were docked five times to ensure consistency in the binding affinity values. The resulting PDBQT files were visualized using Discovery Studio Visualizer v21.1.0.20298 [33] and the ligand interactions between the different receptor models and the PVL ligands, tamoxifen, and estrogen were noted. To automate molecular docking,



python script, PERL script, and windows command prompt were utilized.

Bioisosteric Replacements to Generate Analogs of PVL Ligands

Bioisosteres of PVL ligands which were included in the final list were generated using MolOpt, an open-source web server (https://xundrug.cn/molopt) [33]. The input are SMILES strings and the output are CSV files containing the structures of the bioisosteres as well as the ADMET profile. The web server treats the molecules in two-dimensional configurations; hence, stereoisomers are not recognized. All the bioisosteres generated by the web server were screened by their ADMET profiles. The chosen bioisosteres subjected for molecular docking simulations were nontoxic (liver and kidney cell lines, heart cells, rat, and mouse models) and non-carcinogenic/non -mutagenic, were not substrates/inhibitors/activators of CYP family of enzymes (CYP450 1A2, CYP 450 2C19, CYP450 2C9, CYP450 3A4, CYP 450 2D6), non-inhibitors of p-glycoprotein, and have high intestinal absorption. After the screening, the filtered bioisosteres were then screened again using Swiss ADME to ensure that they have high predicted oral bioavailability. The 2-D structures of the final list of bioisosteres were generated using the Swiss ADME web server [28] and then processed using ChemSketch 2021.1.1 [29]. The 3-D structures were then optimized and the stereoisomers of each bioisostere were generated. The structures of the stereoisomers were 3-D optimized and then subjected to molecular docking simulation. The MOL files output were converted to PDB files using Open Babel.

The final list of bioisosteres which showed comparable binding energies to estrogen and tamoxifen towards the different receptor models were reprocessed using MarvinSketch v21.20.0 [35]. Using this application, 3-D structure optimization was performed to on each structure to find low -energy conformers. Moreover, protonation states of the structures were calculated before doing molecular docking simulations.

Data Analysis

The compounds were grouped according to their compound class which includes flavonoids and phytosterols. The binding energies of the compounds towards each receptor were tabulated and compared. The PDBQT files resulting from the Autodock Vina molecular docking simulation were visualized using Discovery Studio Visualizer v21.1.0.20298 and PyMol v2.5.2 [36]. The ligand-receptor interactions were noted and were related to their binding energies.

Results

The determination of compounds that are found in the edible parts of Phaseolus vulgaris L. (PVL) was conducted through literature search. The initial list contains glycosides that have the same aglycone portion but different sugar moieties. For example, quercetin 3-O-glucoside and quercetin 3-O-rutinoside. In these cases, only one of the compounds was chosen to be part of the list and only the aglycone portion was subjected to screening and molecular docking. Supplementary Table 2 summarizes the secondary metabolites found in PVL. It also includes the plant parts where they were identified, the country of origin, the variety, and the references from where they were lifted. The compound class of secondary metabolites found include flavonoids (flavanone, flavanol, flavone, flavonol, isoflavone, flavononol, anthocyanidin), lignan (isolariciresinol), stilbene (resveratrol), phytosterols (e.g., stigmasterol, betasitosterol), plant hormones (e.g., gibberellins), cinnamic and benzoic acid derivatives (e.g., quinic acid, ferulic acid, hydroxybenzoic acid), and soyasaponins [37-45].

The compounds were screened using ADMETlab 2.0 open web server and the results were summarized in Supplementary Table 3. HIA (human intestinal absorption), bioavailability (E), carcinogenicity/ mutagenicity/ genotoxicity, QED (quantitative estimate of drug-likeness), and Lipinski's rule of five were used as filters. Compounds must have high intestinal absorption (0-0.3) or must have an oral bioavailability of at least 20-30% (0-0.3), must be noncarcinogenic, nonmutagenic, and nongenotoxic, and must be accepted in any of the drug-likeness rules or have QED value of greater than 0 [24]. Moreover, Swiss Target Prediction database (http://www.swisstargetprediction.ch/) was utilized to determine if ER- α is included as a potential target of these compounds.

The secondary metabolites from *Phaseolus vulgaris* L. were then subjected to molecular docking using Autodock Vina v.1.1.2. The final list of compounds which have comparable binding affinities (in kcal per mole) with tamoxifen and estrogen towards the ER-α models (PDB ID: 1A52, 3UUD, 4ZNS, 4ZNV, 5DXE, 5DXG, 5KCD, 5KCT, 5KD9, 5TLT, 5TM8, 5TN4, and 5TN5) were summarized in. The results showed that estrogen exhibits more negative binding affinity across the different receptor models compared to tamoxifen and the PVL compounds. This indicates that estrogen has a better binding affinity than either tamoxifen or PVL compounds. When compared to tamoxifen, most of the PVL compounds exhibit a more negative binding affinity values across the mutant models. On the other hand, tamoxifen outperforms the PVL compounds in terms of



Table 1. Binding Energy Results of Estradiol, Tamoxifen, PVL compounds, and Gibberellin A19 Analogs when Docked to Estrogen Receptors- alpha.

Compound Class	Compound	1A52	3UUD	4ZNS	4ZNV	5DXE	5DXG	5KCD	5KCT	5KD9	5TLT	5TM8	5TN4	5TN5
Endogenous Ligand	Estradiol	-10.7	-10.9	-9.5	-9.6	-11.2	-11	-9.9	-10.2	-10.1	-10.2	-9.6	-9.9	-11.1
SERM	Tamoxifen	-9.3	-5.1	-9.1	-8.6	-4.6	-4.2	-8.8	-9.2	-8.8	-9.3	-9.8	-4.8	-5.0
Flavanone	naringenin	-8.6	-8.0	-8.7	-9.0	-8.0	-7.6	-8.7	-8.8	-8.6	-8.9	-8.6	-8.6	-8.1
	pinocembrin	-8.4	-7.9	-8.1	-8.3	-8.2	-8.0	-8.0	-8.4	-8.4	-7.9	-7.8	-7.5	-8.2
Flavone	apigenin	-8.7	-7.9	-8.8	-9.1	-7.9	-7.5	-8.7	-8.6	-8.7	-8.8	-8.6	-8.5	-8.0
	luteolin	-8.5	-8.0	-8.7	-8.9	-7.8	-7.6	-8.9	-8.8	-8.3	-8.9	-8.3	-8.8	-8.1
Isoflavone	daidzein	-9.1	-8.4	-8.8	-8.9	-8.5	-8.2	-8.9	-8.4	-7.7	-8.5	-8.6	-8.8	-8.5
Flavononol	aromadendrin	-7.9	-7.7	-8.3	-8.6	-7.9	-7.7	-8.3	-8.4	-8.3	-8.6	-8.2	-8.1	-7.9
Anthocyanidins	cyanidin	-9.0	-8.9	-8.7	-8.6	-8.9	-8.8	-8.7	-8.4	-9	-8.8	-8.6	-8.7	-8.7
Phytosterols	beta-sitosterol	-6.8	-3.8	-7.0	-8.0	-2.9	-2.1	-8.0	-8.4	-3.5	-9.3	-7.3	-2.0	-2.7
	campesterol	-7.1	-5.0	-8.1	-8.7	-4.2	-3.4	-7.8	-9.3	-3.3	-10.1	-8.3	-2.3	-3.9
	delta-7 avenasterol	-7.4	-6.0	-7.4	-8.6	-5.6	-4.3	-9.0	-8.8	-2.5	-9.5	-7.8	-3.1	-5.3
	fucosterol	-6.3	-3.7	-7.8	-8.3	-3.0	-1.6	-7.9	-8.5	-4.1	-9.6	-8.2	-1.5	-2.6
	stigmasterol	-6.5	-2.8	-6.4	-8.2	-2.0	-1.1	-8.3	-8.4	-1.6	-8.6	-7.6	-1.6	-1.6
Gibberellin A19	Analog 1	-8.7	-9.1	-8.4	-7.3	-8.8	-8.7	-8.9	-8.2	-8.5	-8.8	-9.1	-8.6	-8.4
Analogs	Analog 2	-7.9	-8.0	-7.3	-7.7	-8.1	-8.1	-8.2	-8.6	-7.3	-8.0	-7.0	-7.4	-7.1
	Analog 3	-8.6	-8.9	-8.3	-7.2	-8.5	-8.4	-8.6	-8.1	-8.5	-8.6	-8.9	-8.4	-8.3
	Analog 4	-8.6	-8.5	-7.6	-7.2	-8.2	-7.8	-9.7	-7.5	-7.4	-9.0	-9.1	-7.5	-7.6

binding affinity on the wild-type ER-α. Tamoxifen's binding affinity, however, tends to become less favorable towards the mutant type of ER- α as seen especially in 3UUD (-5.1 kcal/mol), 5DXE (-4.6 kcal/mol), 5DXG (-4.2 kcal/mol), 5TN4 (-4.8 kcal/mol), and 5TN5 (-5.0 kcal/mol). In contrast, most of the PVL compounds have a consistent binding affinity value towards all the receptor models, both the wild-type and the mutant receptors. Notable deviations were observed with the phytosterols. For example, stigmasterol has a binding affinity of -9.1 kcal/mol in the mutant ER- α 5TLT but has -1.6 kcal/mol binding affinity when docked in the 5TN4 model. The same is true with fucosterol, (-9.6 kcal/mol in 5TLT and – 1.5 kcal/mol in 5TN4), beta-sitosterol (-9.3 kcal/mol in 5TLT and – 2.0 kcal/mol in 5TN4), campesterol (-10.1 in 5TLT and -2.3 kcal/mol in 5TN4), and delta 7-avenasterol (-9.5 kcal/mol in 5TLT and -3.1 kcal/mol in 5TN4). While less favorable binding energies were observed with phytosterols when docked in some of the models, the observed highly negative and comparable binding energies to tamoxifen and estrogen towards the other models, especially the mutant ER- α , cannot be discounted.

Based on the calculated binding energies, none of the PVL compounds nor tamoxifen outperformed estradiol in terms of binding affinity towards the ER-α models. Hence, bioisosteric replacement was used as a strategy to generate analogs of the PVL compounds. MolOpt open web server was utilized to generate the analogs. More than 296,000 bioisosteres were created and from this, 1,572 compounds were subjected to molecular docking. The stereoisomers of these compounds were also generated and were subjected to molecular docking which led to 5,135 compounds. Based on the SWISS ADME Rresults, some PVL compounds have bioiososteres which did not pass the oral bioavailability criteria and were excluded. Only analogs with favorable binding energies (-7.5 kcal/mol) across the different receptors used in this study were considered. Shown in Table 1 are the four gibberellin A19 analogs as well as their binding energies toward the wild-type and mutant receptors.

To determine the amino acid residues that interact with the ligands, the resulting PDBQT files were viewed using Discovery Studio Visualizer v21.1.0.20298. The results are



Table 2. Protein-ligand interactions between Estradiol, Tamoxifen, Phaseolus vulgaris L. compounds, Gibberellin A19 analogs, and the Wild-type ER-α (PDB ID: 1A52).

Compound Class	Compound	Hydrogen Bonding	Hydrophobic Interactions	π- π Stacking Interactions	Miscellaneous interactions	Unfavorable Interactions
Endogenous Ligand	Estradiol	HIS 524	ILE 424, MET 388, LEU 391, LEU 387, ALA 350	PHE 404	-	GLU 353 (unfavorable acceptor- acceptor)
SERM	Tamoxifen	THR 347	ILE 424, MET 388, ALA 350, LEU 525, LEU 391, LEU 387	PHE 404	MET 421(π-S)	-
Flavanone	naringenin	PHE 404, ARG 394	LEU 391, ALA 350, LEU 349, LEU 387, ILE 424	PHE 404	-	-
	pinocembrin	-	LEU 346, LEU 387, ALA 350, LEU 391, LEU 349	PHE 404	GLU 353 (π- anion), MET 421 (π-sulfur)	
Flavone	apigenin	PHE 404, ARG 394	LEU 349, LEU 391, LEU 387, ALA 350, LEU 384	PHE 404	-	-
	luteolin	PHE 404. GLY 521, ARG 394	LEU 349, LEU 391, ALA 350, LEU 387, LEU 384	PHE 404	-	GLU 353 (acceptor- acceptor)
Isoflavone	daidzein	ARG 394, PHE 404, GLY 521, HIS 524	LEU 346, LEU 391, ALA 350, LEU 387, LEU 525	PHE 404	MET 421 (π-S)	GLU 353 (acceptor- acceptor)
Flavononol	aromadendrin	GLU 353, ARG 394, LEU 346, THR 347	MET 421, LEU 387, LEU 391, ALA 350	PHE 404	-	-
Anthocyanidins	cyanidin	-	LEU 387, LEU 391, ALA 350, LEU 525	PHE 404	-	GLU 353 (acceptor- acceptor)
Phytosterols	beta-sitosterol	-	LEU 354, TRP 383, ALA 350, LEU 525, LEU 346	-	-	-
	campesterol	-	TRP 383. ALA 350, LEU 525, LEU 346	-	-	-
	delta-7 avenasterol	-	TRP 383, ALA 350, LEU 525, LEU 346	-	-	-
	fucosterol	-	TRP 383, LEU 525, ALA 350, LEU 346	-	-	-
	stigmasterol	-	LEU 346, ALA 350, LEU 525, TRP 383	-	-	-
Gibberellin A19 Analogs	Analog 1	-	ALA 350, PHE 404, LEU 346	-	-	-
	Analog 2	LEU 346, MET 421, GLU 521	LEU 387, ALA 350, LEU 384, LEU 525	-	-	-
	Analog 3	-	ALA 350, LEU 346, PHE 404	-	-	-
	Analog 4	HIS 524	LEU 525, ALA 350, PHE 404, LEU 346	-	-	-

tabulated in Table 2 and 3. Estradiol (E2) interacts with the wild-type ER- α through H-bonding and hydrophobic interactions. The amino acid residues involved are HIS 524 (H-bonding), ILE 424, MET 388, LEU 391, LEU 387, ALA 350 (hydrophobic interactions), and PHE 404 (π - π stacking). Tamoxifen interacts with the wild-type ER- α through the same types of interactions which involved THR 347 (H-

bonding), ILE 424, MET 388, LEU 391, LEU 387, ALA 350, LEU 525 (hydrophobic interactions), PHE 404 (π - π stacking), and MET 421 (π -S). Unfavorable interaction involving amino acid residue GLU 353 (unfavorable donor-donor) is also present.

Shown in Table 3 are the different amino acid residues of the mutant ER- α (PDB ID: 5TLT) and the different ligands.



Table 3. Protein-ligand interactions between Estradiol, Tamoxifen, Phaseolus vulgaris L. compounds, Gibberellin A19 analogs, and the Mutant ER-α (PDB ID: 5TLT)

Compound Class	Compound	Hydrogen Bonding	Hydrophobic Interactions	π- π Stacking Interactions	Miscellaneous interactions	Unfavorable Interactions
Endogenous Ligand	Estradiol	GLY 521, GLU 353	ILE 424, MET 388, LEU 387, PHE 404, ALA 350, LEU 391	PHE 404	-	-
SERM	Tamoxifen	-	LEU 346, LEU 387, ALA 350, LEU 387, LEU 346, GLY 420, MET 421	PHE 404	MET 421(π-S)	-
Flavanone	naringenin	MET 421, GLU 353, ARG 394	ILE 424, LEU 391, LEU 387, MET 421	PHE 404	-	-
	pinocembrin	MET 421	ALA 350, LEU 346, MET 421, ILE 424	-	-	-
Flavone	apigenin	GLU 353, LEU 387, ARG 394, GLY 521	ALA 350, LEU 391, LEU 387, LEU 384, ILE 424	PHE 404	-	-
	luteolin	GLU 353	ILE 424, MET 421, LEU 391, LEU 387, ALA 350	PHE 404	-	-
Isoflavone	daidzein	GLU 353	LEU 391, LEU 387, ALA 350, LEU 346, LEU 525	PHE 404	-	-
Flavononol	aromadendrin	PHE 425, LEU 387	MET 421, ILE 424, LEU 391, ALA 350, LEU 387	PHE 404	-	ARG 394 (donor- donor)
Anthocyanidins	cyanidin	ARG 394, GLU 353, LEU 346	LEU 391, LEU 387, ALA 350	PHE 404	-	-
Phytosterols	beta-sitosterol	GLU 353	MET 343, MET 388, LEU 384, LEU 387, LEU 391, ALA 350, PHE 404	-	-	-
	campesterol	-	MET 343, LEU 384, LEU 387, ALA 350, LEU 391, PHE 404, MET 388	-	-	-
	delta-7 avenasterol	-	LEU 384, ALA 350, LEU 387, MET 388, LEU 428, LEU 391, MET 421, HIS 524, ILE 424	-	-	-
	fucosterol	HIS 524	LEU 391, LEU 387, ALA 350, LEU 346, LEU 525, MET 528, MET 421, MET 343, HIS 524	-	-	-
	stigmasterol	-	VAL 418, HIS 524, MET 528, MET 343, MET 388, LEU 391, PHE 404, ALA 350, LEU 387	-	-	-
Gibberellin A19	Analog 1	GLU 353	LEU 387, LEU 346, ALA 350	-	-	-
Analogs	Analog 2	GLY 521	LEU 346, LEU 387, ALA 350, LEU 525, LEU 384	-	-	-
	Analog 3	GLU 353	LEU 387, LEU 346, ALA 350	-	-	-
	Analog 4	MET 421, LEU 346	LEU 525, MET 528, ILE 424	-	MET 343 (pi- sulfur)	-

The mutant ER- α 5TLT was used as the representative for the different mutant receptors since the binding of the PVL ligands toward this receptor is the most favorable. Moreover, superimposition of the structures of the different mutant receptors, as shown in Figure 1, indicates that there were no significant differences in their structures and that the ligand binding pocket was preserved. Deviations in the structures of the mutant ER- α models were not within the vicinity of the ligand binding pocket.

For estradiol (E2), most of the interactions involved were hydrogen bonding and hydrophobic interactions. Amino acids GLU 353 and GLY 521 were involved in the hydrogen bonding interactions between estrogen and the wild-type and mutant ER- α . For hydrophobic interactions, the amino acids involved were ILE 424, MET 388, LEU 387, PHE 404, ALA 350, and LEU 391. The amino acid PHE 404 was also involved in π - π stacking interactions. Tamoxifen interacted with the ER- α by hydrogen bonding through the amino acid



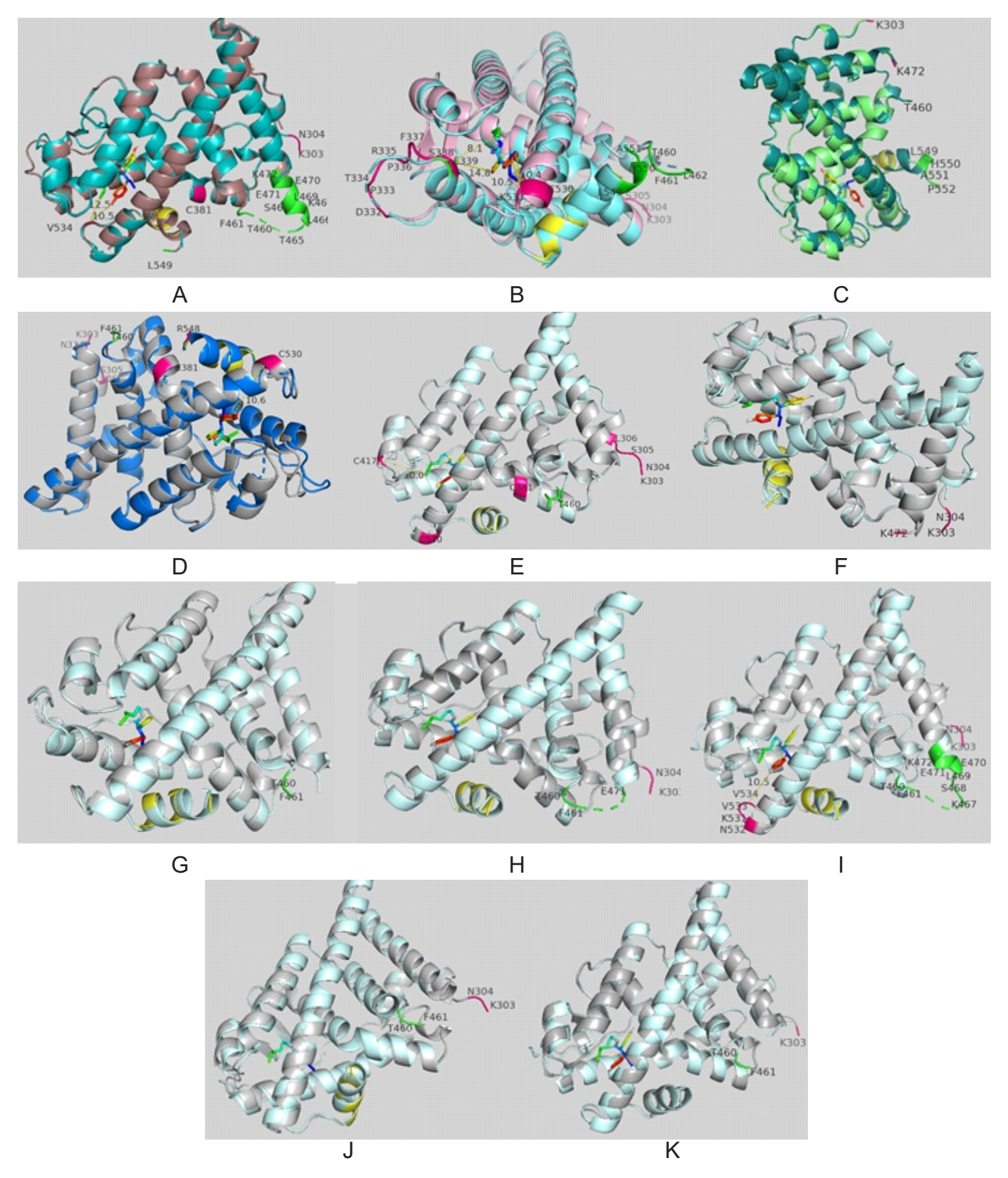


Figure 1. Superimposed structures of the mutant receptors with the ER-α PDB ID: 5TLT as the reference receptor. A) PDB ID: 3UUD, B) PDB ID: 4ZNS, C) PDB ID: 4ZNV, D) PDB ID: 5DXE, E) PDB ID: 5DXG, F) PDB ID: 5KCD, G) PDB ID: 5KCD, H) PDB ID: 5KCT, I) PDB ID: 5TM8, J) PDB ID: 5TN4, K) PDB ID: 5TN5. Labeled also are the amino acid residues that are different between the structures. The perturbation closest to the ligand-binding cleft can be seen in B which is 8 Å involving E338 residue. Shown also in rainbow is 7ED, an investigational SERM which is the co-crystallized ligand of the ER-alpha PDB ID: 5TLT. The structure highlighted in yellow is helix 12, an essential part of the 3D structure of the ER-alpha involved in the activation of the receptor into agonist form. The calculated RMSD values of the superimposed receptors with respect to 5TLT are less than 2 Å.



THR 347 in the wild-type ER- α whereas in the mutant receptor, this was absent. Hydrophobic interactions were also responsible for most interactions between tamoxifen and the estrogen receptors. Several amino acids were involved in the said hydrophobic interactions which were LEU 346, LEU 387, ALA 350, LEU 387, LEU 346, GLY 420, and MET 421. Like in the case of E2, PHE 404 was involved in π - π stacking interactions and a miscellaneous interaction involving MET 528 through pi-sulfur interaction is also present.

The PVL compounds interacted with the wild-type ER- α mostly through hydrophobic interactions which involved ALA 350, GLU 353, GLY 521, HIS 524, ILE 424, LEU 384, LEU 346, LEU 387, LEU 391, LEU 349, LEU 384, LEU 387, LEU 391, LEU 525, MET 343, MET 388, MET 421, MET 522, PHE 404, AND and TRP 383. Π - π stacking interactions which involved PHE 404 is were also observed between the wild-type ER- α and all the flavonoids. Hydrogen bonding is also a type of interaction present between the flavonoids and the wild-type receptor which often involves the amino acid residues HIS 524, ARG 394, GLU 353, PHE 404, and GLY 521.

As with the case of the other compounds, most interactions present between gibberellin A19 analogs, and the estrogen receptors alpha were hydrogen bonding and hydrophobic interactions. These involved amino acids GLU 353 and GLY 521 for H-bonding whereas ALA 350, LEU 525, and LEU 384 were some of the amino acids involved in hydrophobic interactions.

In Table 4, the structures, molecular formula, molecular weight, and the synthesizeability scores of the analogs are shown. Presented in Table 5 are their absorption, distribution, metabolism, and excretion profiles are presented. 'Pgp-inh' stands for p-glyocprotein inhibitor, 'pPgp-sub' for pglycoprotein substrate, 'HIA' for human intestinal absorption, 'F' for oral bioavailability, 'BBB' for blood -brain barrier, 'PPB' for plasma protein bound, and 'CL' for clearance. The values are given as probability. For the absorption and distribution, the values are given as the probabilities of being a pPgp-inh, being pPgp-sub, and being poorly absorbed; probability of having an oral bioavailability of less than 20% or 30%, probability of not penetrating the blood -brain barrier, and the percentage of being protein bound. Hence, for Pgp-inh, Pgp, sub, HIA, and F, values within the range of 0-0.3 are desirable while for BBB, a value of 0.7 to 1.0 is desirable in the context of this study. For PPB, values less than or equal to 90% are desirable and for clearance (CL), values greater bound within 5 are preferred. In Table 6, the metabolism profile of the analogs is presented. Given in each column are the family

of cytochrome enzymes and the probabilities of being a substrate or inhibitor. As much as possible, it is desirable that the probability values are from 0 to 0.7. For the toxicity profile given in Table 7, the columns represent human ether-a-go-go related gene toxicity (hERG), human hepatotoxicity (H-HT), drug-induced liver injury (DILI), Ames toxicity, rat oral toxicity (ROA), carcinogenicity, respiratory toxicity, probability to bind to androgen receptor (NR-AR), probability to bind to androgen receptor ligand-binding domain (NR-AR-LBD), probability to act as aromatase inhibitor (NR-aromatase), probability of binding to estrogen receptor (NR-ER), and estrogen receptor ligand-binding domain (NR-ER-LBD). For the context of this study, values ranging from 0 to 0.3 are desirable for hERG, H-HT, DILI, Ames, ROA, carcinogenicity, and respiratory columns. For the rest of the columns, values higher than 0.3 are preferred [34].

Discussion

 $ER-\alpha$ has been established to be involved in cancer progression and metastases. One mechanism is through mutation in the ligand binding domain of the receptor [8,46,47]. The most common and most invasive of which is the Y537S type [48,49]. In this study, the crystal structures of the wild-type ER-α (PDB ID: 1A52) and the 12 mutant estrogen receptors alpha of the Y537S type (PDB ID: 3UUD, 4ZNS, 4ZNV, 5DXE, 5DXG, 5KCD, 5KCT, 5KD9, 5TLT, 5TM8, 5TN4, and 5TN5) were used in in silico screening of PVL compounds as potential anticancer agents. The presence of Y537S mutation makes the receptor constitutively active, independent of the native ligand estradiol. In the agonist conformation, the helix 12 (H12) rests across H3 and H11 to form an indentation which accommodates co-regulator binding [50]. This structural feature is seen in Figure 2. Note that 1ERE (wild-type and in agonist conformation) was utilized instead of 1A52 (wild-type and in agonist conformation) to compare the structural features since the helix 12 of the former is more exemplified than the former. Hence, superimposing the structures make the visualization easier.

The Y537S mutation also results to in the replacement of Y537-N348 interaction with S537-D351 hydrogen bonding which optimizes the H11-H12 loop in the agonist conformation allowing the coactivators to be recruited to the AF2 cleft. The stabilization of the agonist conformation also reduces the affinity of tamoxifen towards the receptor [51]. This is evident when tamoxifen was docked in the mutant receptors 3UUD, 5DXE, and 5DXG as compared to the wild-type receptor 1A52. In these mutant receptors, estradiol is the co-crystallized ligand, hence the receptor is in the agonist



 Table 4. Swiss ADME results of the Gibberellin A19 analogs

Molecule	ADME results of the Formula	e Gibberellin A19 a MW (g/mol)	nalogs Synthetic Accessibility	Structure
Analog 1	$C_{20}H_{26}FO_5$	365.42	5.54	
Analog 2	$C_{20}H_{26}O_6$	362.42	5.41	
Analog 3	C ₂₀ H ₂₅ FO ₅	366.42	5.57	
Analog 4	$C_{23}H_{29}NO_4$	383.48	5.4	



Table 5. Absorption, distribution, and excretion profile of Gibberellin A19 analogs obtained from the ADMETlab2.0 web server

Compound			Absorption			Distri	bution	Excretion
	Pgp-inh	Pgp-sub	HIA	F(20%)	F(30%)	BBB	PPB	CL
Analog 1	0	0.964	0.015	0.89	0.556	0.836	52.86%	2.224
Analog 2	0.001	0.01	0.04	0.952	0.101	0.828	58.67%	1.005
Analog 3	0	0.964	0.015	0.89	0.556	0.836	52.86%	2.224
Analog 4	0	0.784	0.005	0.133	0.014	0.912	49.19%	2.496

Table 6. Metabolism profile of Gibberellin A19 analogs obtained from the ADMETlab2.0 web server

Compound		Metabolism										
	CYP1A2-inh	CYP1A2-sub	CYP2C19-inh	CYP2C19-sub	CYP2C9-inh	CYP2C9-sub	CYP2D6-inh	CYP2D6-sub	CYP3A4-inh	CYP3A4-sub		
Analog 1	0.002	0.925	0.007	0.239	0.005	0.053	0.004	0.069	0.758	0.075		
Analog 2	0.001	0.754	0.008	0.083	0.01	0.119	0.007	0.083	0.242	0.013		
Analog 3	0.002	0.925	0.007	0.239	0.005	0.053	0.004	0.069	0.758	0.075		
Analog 4	0.004	0.889	0.014	0.128	0.012	0.097	0.013	0.084	0.844	0.12		

Table 7. Toxicity profile of Gibberellin A19 analogs obtained from the ADMETlab2.0 web server

Compound		Toxicity Profile											
	hERG	н-нт	DILI	Ames	ROA	Carcinogenicity	Respiratory	NR-AR	NR- Aromatase	NR-ER	NR-ER- LBD		
Analog 1	0.022	0.698	0.037	0.067	0.791	0.665	0.985	0.949	0.844	0.533	0.008		
Analog 2	0.01	0.183	0.054	0.02	0.101	0.14	0.839	0.882	0.619	0.387	0.01		
Analog 3	0.022	0.698	0.037	0.067	0.791	0.665	0.985	0.949	0.844	0.533	0.008		
Analog 4	0.035	0.665	0.033	0.03	0.943	0.587	0.985	0.968	0.919	0.899	0.102		

conformation. However, the binding affinities of tamoxifen towards 3UUD, 5DXE, and 5DXG have significantly decreased as compared to its binding affinity towards 1A52 as shown in Table 1. This is also evident in Figure 3A, wherein the structure of the wild-type ER-α bound to 4-hydroxytamoxifen (PDB ID: 3ERT), a SERM, was superimposed to the structure of the mutant ER-α bound to 7ED (PDB ID: 5TLT), an investigational SERM. Note that 3ERT was utilized for visualization of the antagonist conformation of the wild-type receptor and not in the molecular docking experiment. Highlighted in the structures is the helix 12 of the receptors. The image shows that the helix 12 (green and violet), which is crucial in the agonist-antagonist switching of the receptor, does not overlap. If both structures bind SERM, they should be in the antagonist conformation but that is not the case in 5TLT. Moreover, to exemplify the stabilization of the agonistic form in mutant receptors, the structure of wild-type ER-α bound to estrogen (PDB ID: 1ERE) is overlayed to the structure of mutant ER-α 5TLT in Figure 3B. As shown, the helix 12 (red

and green) of the structures overlapped, indicating that 5TLT is in agonistic conformation despite being bound to 7ED.

As previously mentioned, 5TLT was used as the mutant receptor reference. Figure 3 shows the image of the overlapped structures. In all the mutant receptors structures, the helix 12 overlapped. Moreover, the differences in the amino acid residues in the mutant estrogen receptors alpha are also labeled. The RMSD values between the 5TLT structure and the other mutant receptors are below 2 Å. The RMSD value indicates the average deviation between corresponding atoms of two proteins and that the smaller the value, the higher is the similarity [52]. Moreover, the deviations in the amino acid residues in the structure do not directly interact within the ligand binding pocket. The closest possible nonbonding interaction to the deviation in amino acid residue is 8.1 A as shown in Figure 1. This distance is large even for an effective hydrophobic interaction (5.5 A) or any unfavorable interactions (5.6 A) [33]. Additionally, the ligand



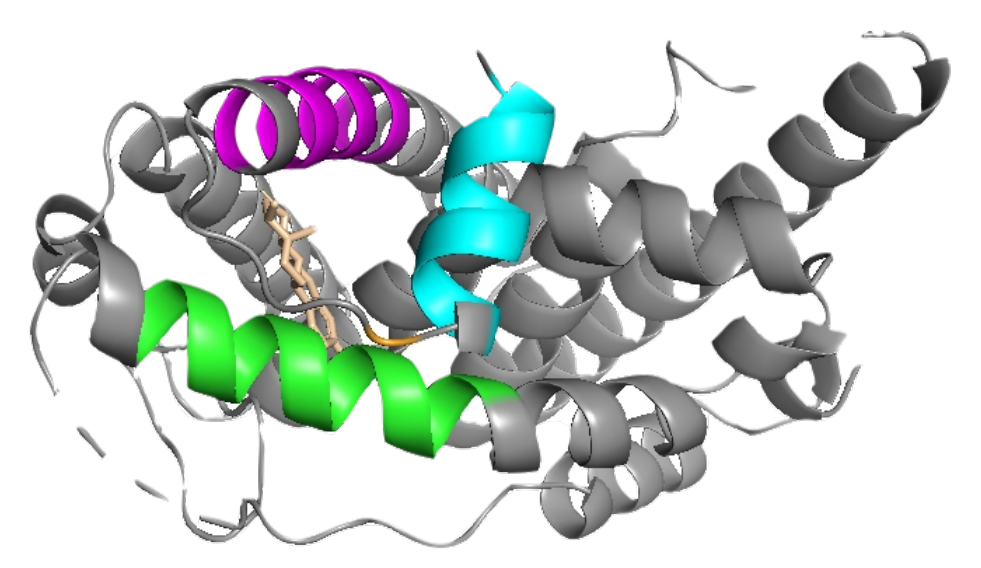


Figure 2. Structure of wild-type ER-α (PDB ID: 1ERE). Highlighted in cyan is helix 12, in purple is helix 11 and in green is helix 3. The co-crystallized ligand E2 is also shown in cream. Shown here is helix 12 resting over helices 11 and 3 which stabilizes the agonist conformation.

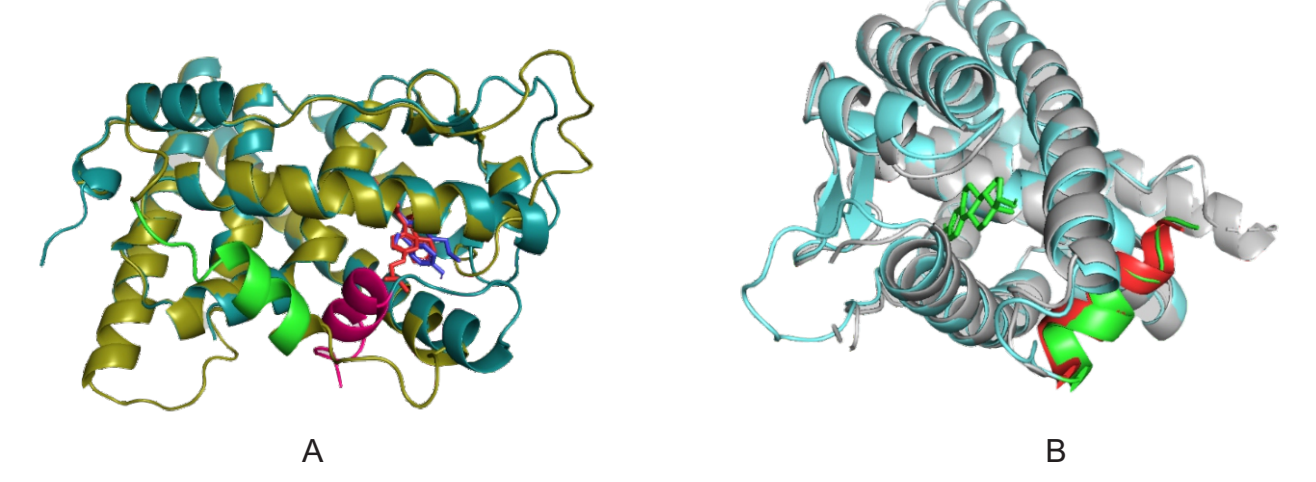


Figure 3. Superimposed structures of the A) wild-type ER- α (PDB ID: 3ERT) (olive green) bound to tamoxifen and mutant ER- α (light blue) bound to 7ED (PDB ID: 5TLT) and B) Image of superimposed mutant ER- α 5TLT (light blue) and wild-type ER- α 1ERE (gray) bound to estradiol.

binding pocket is formed by parts of helices 3, 6, 8, and 11, and 12 and S1/S2 hairpin involving the amino acid residues MET 342 to LEU 354, TRP 383 to ARG 394, VAL 418 to LEU 428 and MET 517 to MET 528, LEU 539 to HIS 547 and LEU 402 to LEU 410 [53,54] and the deviations in amino acid residues are not found within these helices. Since a rigid receptor-flexible ligand type of molecular docking was conducted, the differences in the binding affinity values across the different mutant receptors can be attributed mainly to the structures of the ligands and the scoring function of Autodock Vina [55].

Table 2 and Table 3 show that there are similarities in the interacting amino acids between the ER- α , the endogenous

ligand estradiol, the SERM tamoxifen, as well as the PVL ligands. This, in addition to the favorable binding energies across the different mutant receptors and the wild-type receptor presented in suggests the ability of PVL compounds to act either as agonist or antagonist [50,56]. The similarity in structure between E2 and flavonoids allows the latter to act as ER-α modulators. The distance between the hydroxyl groups and the phytoestrogens is almost the same, at 14.5 A [57]. Moreover, the 4'-OH group of the flavonoids binds in the same way as the ring A of E2, forming hydrogen bonds with the residues GLU 353 and ARG 394 [58]. Lee and Barron (2017) mentioned that THR 347 and HIS 524 are also involved in hydrogen bonding and overall, these interactions help in



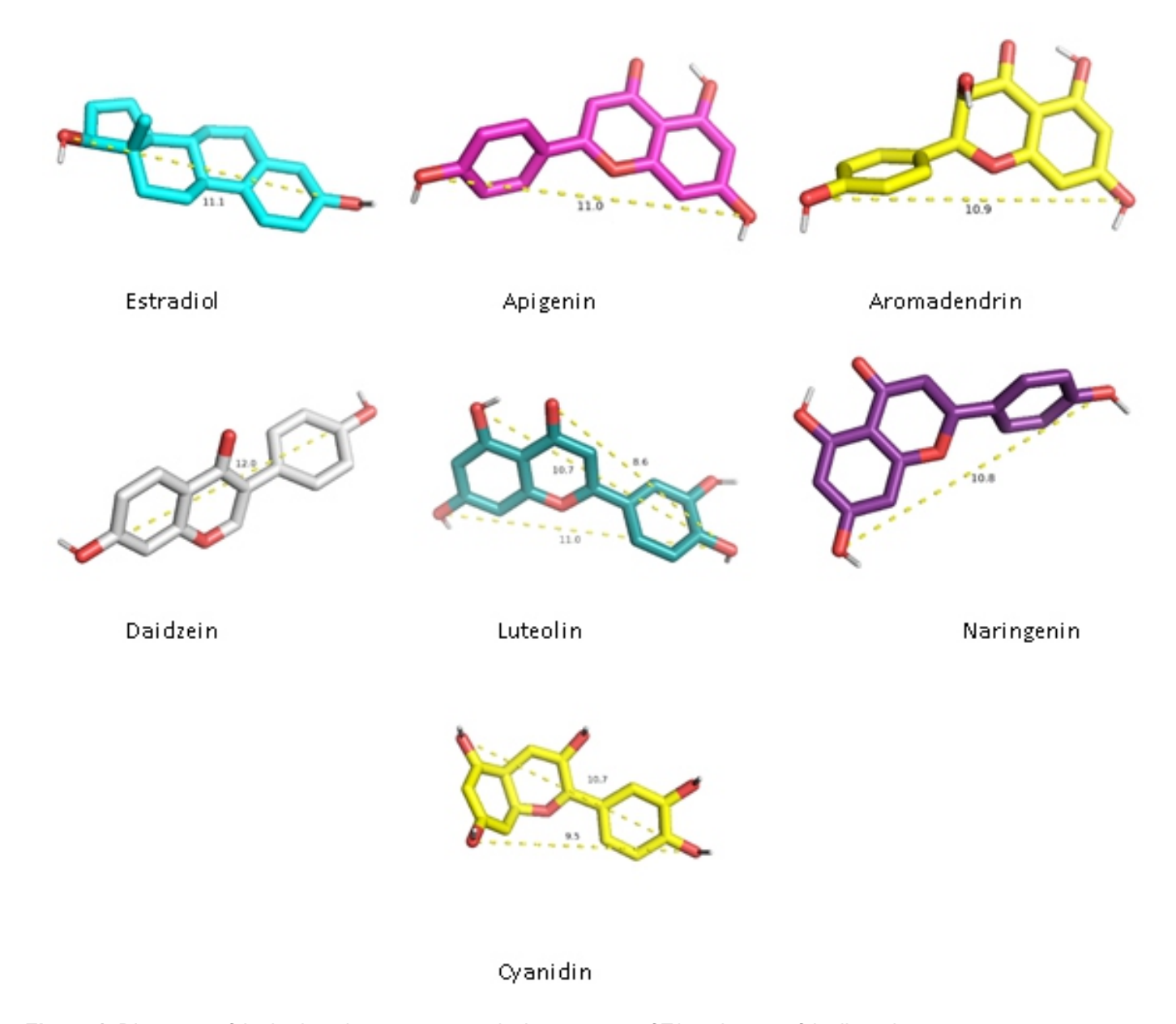


Figure 4. Distances of the hydroxyl groups present in the structure of E2 and some of the ligands.

attaching the ligand in the ligand binding pocket [59]. The distance obtained in E2 is 11.1 A and the rest of the compounds have the distances of their hydroxyl groups (4'-OH phenyl hydroxyl and OH at position 6) around this value (9-12 A) (Figure 4).

Aside from hydrogen bonding, hydrophobic forces make up majority of the protein-ligand interactions. This occurs via the phenyl group, like the ring A of E2. The presence of the aromatic ring is also a characteristic of a good ligand for ER alpha [59]. and this is present also in the structures of PVL flavonoids. In the interaction analysis of synthesized coumarin derivatives conducted by Shylaja *et al.* (2021) [26], involving

the same receptors (wild-type and mutant receptors), PHE 404 via π - π stacking interactions is present when ER alpha interacts with an agonist. This type of interaction involving PHE 404 can be seen in the flavonoids found in PVL compounds. Moreover, in the same study, the other amino acid residues involved in hydrophobic interactions involves HIS 524, ILE 424, LEU 428, LEU 391, and LEU 346. Interactions between these amino acid residues is are essential to stabilize H3 and H11 in agonist conformation since these hydrophobic interactions hold H11, H8, H6, beta-sheet, and H3 together. In Table 2 and Table 3, these amino acid residues are also the recurring amino acids that are present in the hydrophobic interactions between the flavonoids of PVL and the ER alpha.



These same interactions are also present in the phytosterols. This strengthens the idea that the flavonoids, which are also phytoestrogens, can bind and modulate ER- α activity in both wild-type and mutant receptors.

In the macromolecule-ligand-complex based pharmacophore modeling conducted by Shylaja et al. (2021) using the same mutant receptors, they found that the pharmacophoric features of good ligands for these ER-α receptors possess two aromatic rings, a hydrogen bond acceptor or donor and hydrophobic features [26]. All the flavonoids found to be present in PVL possess these characteristics. The structures of flavonoids found in PVL contain two aromatic ring moieties, possible hydrogen bond donors and acceptors, and hydrophobic moieties. This further explains the favorable interactions and binding affinities observed with flavonoids when docked in the ER- α receptors. The results of the current study are also in coherence with the results obtained by D'Arrigo et al. (2021) [60] which involved apigenin, genistein, luteolin, naringenin, quercetin, and resveratrol [60]. In their study, these six flavonoids were docked in nuclear receptors including ER-α and the compounds showed good docking scores and complementarity with the ER- α and ERbeta. Their study also showed that E2 obtained the most favorable binding score.

In an *ex vivo* experiment conducted by Chen and Chien (2019) [61] which utilized breast cancer cells from breast cancer patients, and involved genistein, resveratrol, and quercetin, it was found that the phytoestrogens inhibit human breast cancer viability [61]. Moreover, proteins involved in the apoptotic pathway and estrogen receptor beta were increased in cells that were treated with phytoestrogens. These results suggest that the flavonoids have potential antibreast cancer capabilities. Certainly, the ability of flavonoids to act against breast cancer has been widely studied in literature [23,60-62].

While the agonistic interactions between the ER- α (wild-type and mutant) are present, Tables 4 and 5 shows that the amino acid residues involved in the interaction of tamoxifen with the ER- α receptors are also like that of the interaction between PVL ligands and the receptors. This similarity in amino acid residues suggests that the PVL compounds can also interact with ER- α in an antagonistic manner. Shylaja *et al.* (2021) identified four hydrophobic holes that are present within the ligand binding pockets which involved LEU 384: LEU 387: LEU 391 (hydrophobic hole 1), PHE 404: ILE 424 (hole 2), LEU 349: ALA 350 (hole 3), and, MET 343: LEU 346, LEU 525 (hole 4) [26]. All these amino acids are present in the interaction between the flavonoids in PVL as well as the

phytosterols. These protein-ligand interactions indicate that the flavonoids, lignan, and stilbene (phytoestrogens) can also act as an antagonist. The agonistic and antagonistic activities of these phytoestrogens are beneficial when there is a deficiency in estrogen levels or overexpression of estrogen receptors [57].

Another class of compound found in PVL are is the phytosterols. Their core structure is cholesterol which is also a precursor for the biosynthesis of E2 in the human body [65]. Plant sterols are known to exhibit anticancer properties [66]. A phytosterol, beta-sitosterol, is also considered as a phytoestrogen and has been shown in vitro to competitively bind to ER- α [65]. As seen in Table 2 and Table 3, the phytosterols present in PVL bind favorably, to some extent, to both the wild-type and mutant estrogen receptors alpha. This suggests a possible competitive binding or even an agonistic binding. This idea is strengthened by the fact that the amino acid residues involved in the interaction between E2 and the ER-α receptors as well as between the phytosterols and the receptors, both the wild-type and the mutant receptor have some degree of similarities as shown in Table 2 and 3. As previously mentioned, there were instances wherein the binding of phytosterols toward the mutant receptors is unfavorable. It should be noted that while there is no significant difference between the structures of the mutant receptors used in the study (RMSD < 6.0 A), it is not equal to zero. This suggests that these fine differences (which may include distances among the different residues and the spatial orientation) may have contributed to these deviations [33]. Moreover, an examination of the structures of phytosterols reveals that there are various rotatable bonds present in the side chains which may orient itself in different ways towards the receptor which may lead to less favorable binding energies. In a quantitative structure activity relationship study conducted by Gao et al. (1999) involving estrogen receptor and its ligands, they found that the receptor has limited tolerance to steric effects at the number 16 position of estradiol [66]. If the structure of the phytosterols and E2 are compared, this position is in proximity with to the position 17 where the side chains of the phytosterols are situated. This supports the idea that steric clashes from the phytosterols result to in unfavorable binding. Moreover, in the Autodock Vina Program, the presence of steric effects and steric and hydrophobic interactions, based on the weighted scoring function utilized, results to in a less negative binding score [32].

Of all the analogs generated, only those of the gibberellin A19 bioisosteres were found to have favorable interactions across the different ER- α models and were found to have



good ADMETox profile from the MolOpt web server. Analogs of gibberellin A19 were summarized in Table 4.

These analogs have comparable binding affinity across the different estrogen receptors alpha with respect to E2 and tamoxifen. The structures of the analogs are shown in Table 4, whereas their interactions with the amino acid residues of ER are summarized in Table 2 and Table 3. As seen in the table, the amino acid residues have some similarityies with the amino acid residues interacting with both E2 and tamoxifen. Specifically, ARG 394, GLU 353, and HIS 524 are all involved in hydrogen- bonding whereas amino acids like LEU 540, LEU 525, ALA 350, LEU 346, PHE 404, and MET 388 are involved in hydrophobic interactions. While there are similarities, it should be noted that the structures contain an acidic moiety which becomes protonated once it reaches the target site of the microtumor environment. MarvinSketch v21.20.0 reveal that the acidic moieties have ha pKa of about 4.6. Hence, it is most likely to be in the deprotonated state at the target site since the pH of the microtumor environment is around 6.7 [69]. This poses a problem since the target, ER- α , are is mostly situated inside the cell, particularly the nucleus. It will be difficult for the analogs to penetrate the cell since they will be in their charged form, unless there are cellular transporters which can recognize these analogs and transport them inside the cell [70]. The presence or absence of transporters for the analogs is beyond the scope of this paper.

ADMETlab 2.0 results of the gibberellin A19 analogs presented in Table 7 reveal that these analogs are predicted to have high intestinal absorption but low oral bioavailability. They all passed the Lipinski's rule of 5 drug-likeness rules. Also, as predicted in their structure (highly polar because of the carboxylic acid moiety, fluorine, hydroxyl groups, carbonyl carbon, negative charges), they cannot cross the blood -brain barrier, suggesting that they may not cause neurologic side effects, unlike other anticancer drugs which cause central or peripheral nervous system complications [71]. All of them have less interactions with the CYP enzymes indicating that the first pass metabolism or drug interactions may be lessened or avoided. First pass metabolism and pharmacokinetic drug interactions may lessen the drug in the site of action, making it less effective or may heighten toxic effects [72-74]. The Swiss ADME web server also predicted that there will be some difficulty in synthesizing these compounds since they obtained a score of a little over 5. In the Swiss ADME training data sets, a score of 10 indicates a very difficult synthesizability whereas a score of 1 indicates otherwise [28].

Based on the ADMETlab2.0 results presented in Table 5, the gibberellin A19 analogs are most likely to be substrates of p-glycoprotein. This will become a problem later because p-glycoproteins are part of efflux mechanisms of cancer cells which lead to treatment resistance [75]. Since the PPB (plasma protein binding) percentage is less than 90%, they are predicted not to be highly protein bound. This is a good characteristic of the analogs because highly protein -bound drugs tend to have a low therapeutic index. For the excretion profile, the clearance probabilities are given in Table 5. Since the value is less than 5, they are predicted to exhibit low clearance. This has implications in the frequency dosing of the compounds since frequent dosing with low clearance of the drugs can induce toxic side- effects. This agrees with their metabolism profile (Table 6) since they interact less with the CYP enzymes except in some instances such as that of analog 1 and its protonated analog 3 which are predicted to be substrates of CYP1A2. These two compounds are also predicted to be CYP3A4 inhibitors. This prediction leads to the idea that they tend to undergo first pass metabolism and the amount of the intact compound which goes to the target site is decreased [72].

Table 7 shows that the compounds show hepatotoxicity (H-HT probability score > 0.3) and moderate carcinogenicity except for Analog 2 (probability score is 0.14< 0.3). They are predicted to test negative in the Ames test and all of them are predicted to be orally toxic when administered to rats except for analog 2. Moreover, all of them are predicted to be highly toxic in to the respiratory system (probability score > 0.3). They are, however, not cardiotoxic (hERG probability score < 0.3). It is noteworthy that they are predicted to bind to the androgen receptors, aromatase enzyme, and estrogen receptor (probability scores > 0.3). As previously discussed, these receptors and enzymes play a crucial role in the pathogenesis of breast cancer and the ability of these compounds to be act as ligands to these proteins may suggest that they can act as either agonist, antagonist, or receptor modulators. Nevertheless, as predicted in their structures, the compounds will have difficulty reaching the ligand-binding domain of the estrogen receptor as supported by the low probability in the NR-ER-LBD column of Table 7 [24]. These constellations of results suggest that further optimization of the analogs should be done to improve their ADMET profiles.

Conclusion

Phaseolus vulgaris L. (fam. Fabaceae) contains compounds which belong to the group of phytoestrogens, phytosterols,



and plant hormones. The phytoestrogens, phytosterols, and plant hormone analogs show favorable binding affinity towards the wild-type $ER-\alpha$ and the mutant receptors of Y537S type. The most common interactions between E2, tamoxifen, and the PVL ligands were found to be hydrogen bonding, hydrophobic, and π - π stacking interactions. The similarities in the amino acid residues that interact with E2, tamoxifen, and the PVL ligands in addition to the favorable binding energies, suggest that these compounds are possible candidates against ER-positive breast cancer. The compounds and analogs presented in this work can be further optimized to obtain compounds which can outperform E2 in terms of binding and activity towards ER-α, especially the mutant types. Moreover, molecular dynamics simulation, and in vitro tests can be conducted to surpass the limitations of the current study.

References

- Comsa S, Cimpean A, Raica M. (2015) 'The Story of MCF-7 breast cancer cell line: 40 Years of experience in research'. Anticancer Research 35:3147-3154.
- 2. World Health Organization. (2021) Breast Cancer.
- 3. World Health Organization. (2021) Cancer Today.
- 4. Laudico A, Mirasol-Lumague M, Medina V, Mapua C, Valenzuela F, Pukkala E. (2015) Philippine Cancer Facts and Estimates . Philipp Cancer Soc. 1-79.
- 5. Shah R, Rosso K, Nathanson D. (2014) 'Pathogenesis, prevention, diagnosis and treatment of breast cancer'. World Journal of Oncology, 5(3):283-298.
- 6. Kosir A. (2019) Breast Cancer.
- Wen C, et al. (2017) 'Unifying mechanism in the initiation of breast cancer by metabolism of estrogen (review)'. Molecular Medicine Reports 16, 1001-1006.
- Padrão NA, Mayayo-Peralta I, Zwart, W. (2020)
 Targeting mutated ER-α: Rediscovering old and identifying new therapeutic strategies in metastatic breast cancer treatment. Current Opinion in Endocrine and Metabolic Research, 15, 43–48. doi: 10.1016/j.coemr.2020.10.008.
- Waks AG, Winer EP. (2019) Breast Cancer Treatment: A Review. JAMA, 321(3):288–300. doi: 10.1001/jama.2018.19323.
- Dustin D, Gu G, Fuqua SAW. (2019) ESR1 mutations in breast cancer. Cancer, 125(21):3714–3728. doi: 10.1002/cncr.32345.
- Godone R, Leitão GM, Araújo NB, Castelletti C, Lima-Filho JL, Martins D. (2018) Clinical and molecular aspects of breast cancer: Targets and

- therapies. Biomedicine & pharmacotherapy = Biomedecine & pharmacotherapie, 106:14–34. doi: 10.1016/j.biopha.2018.06.066.
- 12. Deepak K, Vempati R, Nagaraju GP, Dasari VRSN, Rao D, Malla RR. (2020) Tumor microenvironment: Challenges and opportunities in targeting metastasis of triple negative breast cancer. Pharmacological Research, 153, 104683. doi: 10.1016/j.phrs.2020.104683.
- 13. Joshi H, Press MF. (2018) Molecular Oncology of Breast Cancer. The Breast, 282–307.e5. doi: 10.1016/b978-0-323-35955-9.00022-2.
- Huang B, Warner M, Gustafsson J. (2014) 'Estrogen receptors in breast carcinogenesis and endocrine therapy'. Molecular and Cellular Endocrinology. doi: 10.1016/j.mce.2014.11.015.
- 15. Reinert T, Saad ED, Barrios CH, Bines J. (2017) Clinical Implications of ESR1 Mutations in Hormone Receptor-Positive Advanced Breast Cancer. Frontiers in oncology, 7, 26. doi: 10.3389/fonc.2017.00026.
- 16. Lei JT, Gou X, Seker S, Ellis MJ. (2019) ESR1 alterations and metastasis in estrogen receptor positive breast cancer. Journal of cancer metastasis and treatment, 5(38). doi: 10.20517/2394-4722.2019.12.
- 17. Thompson MD, Thompson HJ, Brick MA, McGinley JN, Jiang W, Zhu Z, Wolfe P. (2008) Mechanisms associated with dose-dependent inhibition of rat mammary carcinogenesis by dry bean (*Phaseolus vulgaris* L.) The Journal of nutrition, 138(11):2091–2097. doi: 10.3945/jn.108.094557.
- 18. Campos-Vega R, Guevara-Gonzalez R, Guevara-Olvera B, Dave Oomah B, Loarca-Piña G. (2010) Bean (*Phaseolus vulgaris* L.) polysaccharides modulate gene expression in human colon cancer cells (HT-29) Food Research International, 43(4):1057–1064. doi: 10.1016/j.foodres.2010.01.017.
- Lam SK, Ng TB. (2011) Apoptosis of human breast cancer cells induced by hemagglutinin from *Phaseolus* vulgaris cv. Legumi secchi. Food Chemistry, 126(2):595–602. doi: 10.1016/j.foodchem.2010.11.049.
- 20. Luna-Vital DA, et al. (2014) 'Biological potential of protein hydrosylates and peptides from common bean (*Phaseolus vulgaris* L.): A Review'. Food Research International doi: 10.1016/j.foodres.2014.11.024.
- 21. Donoso-Quezada J, Guajardo-Flores D, González-Valdez J. (2020) Enhanced exosome-mediated delivery of black bean phytochemicals (*Phaseolus vulgaris* L.) for cancer treatment applications. Biomedicine & Pharmacotherapy, 131, 110771.



- Abu-Reidah I, et al. (2012) 'Phytochemical characterisation of green beans (*Phaseolus vulgaris* L.) by using high-performance liquid chromatography coupled with time-of-flight mass spectrometry'. Phytochemical Analysis doi: 10.1002/pca.2385.
- 23. Dixon RA. (2004) PHYTOESTROGENS. Annual Review of Plant Biology, 55(1):225–261. doi: 10.1146/annurev.arplant.55.031903.141729.
- 24. Xiong G, Wu Z, Yi J, Fu L., Yang Z, Hsieh C, Yin M, Zeng X, Wu C, Lu A, Chen X, Hou T, Cao D. (2021) ADMETlab 2.0: an integrated online platform for accurate and comprehensive predictions of ADMET properties. Nucleic Acids Research, 49(W1):W5–W14. doi: 10.1093/nar/gkab255.
- 25. Pavlin M, Spinello A, Pennati M, Zaffaroni N, Gobbi S, Bisi A, Colombo G, Magistrato A. (2018) A Computational Assay of Estrogen Receptor α Antagonists Reveals the Key Common Structural Traits of Drugs Effectively Fighting Refractory Breast Cancers. Scientific reports, 8(1):649. doi: 10.1038/s41598-017-17364-4.
- 26. Shylaja R, Loganathan C, Kabilan S, Vijayakumar T, Meganathan C. (2021) Synthesis and evaluation of the antagonistic activity of 3-acetyl-2H-benzo[g]chromen-2-one against mutant Y537S ER-α via E-Pharmacophore modeling, molecular docking, molecular dynamics, and in-vitro cytotoxicity studies. Journal of Molecular Structure, 1224, 129289. doi: 10.1016/j.molstruc.2020.129289.
- 27. Kim S, Chen J, Cheng T, Gindulyte A, He J, He S, Li Q, Shoemaker BA, Thiessen PA, Yu B, Zaslavsky L, Zhang J, Bolton EE. (2019) PubChem in 2021: new data content and improved web interfaces. Nucleic Acids Res., 49(D1):D1388–D1395. doi: 10.1093/nar/gkaa971.
- Daina A, Michielin O, Zoete V. (2017) Swiss ADME: a free web tool to evaluate pharmacokinetics, drug-likeness and medicinal chemistry friendliness of small molecules. Scientific Reports, 7(1) doi: 10.1038/srep42717.
- 29. ACD/ChemSketch, version 2021.1.1, Advanced Chemistry Development, Inc., Toronto, ON, Canada, www.acdlabs.com, 2022.
- 30. Forli S, Huey R, Pique ME, Sanner MF, Goodsell DS, Olson AJ. (2016) Computational protein-ligand docking and virtual drug screening with the AutoDock suite. Nature protocols, 11(5):905–919. doi:10.1038/nprot.2016.051.
- 31. N M O'Boyle, M Banck, C A James, C Morley, T Vandermeersch, G R Hutchison. (2011) "Open Babel: An open chemical toolbox." J. Cheminf.: 3(33). DOI:10.1186/1758-2946-3-33.
- 32. Trott O, Olson AJ. (2010) AutoDock Vina: improving

- the speed and accuracy of docking with a new scoring function, efficient optimization, and multithreading. Journal of computational chemistry, 31(2): 455–461. doi: 10.1002/jcc.21334.
- 33. BIOVIA, Dassault Systèmes, [Discovery Studio Visualizer], [v21.1.0.20298], San Diego: Dassault Systèmes, [2021].
- 34. Shan J, Ji C. (2020) MolOpt: A Web Server for Drug Design using Bioisosteric Transformation. Current Computer-Aided Drug Design, 16(4): 460–466. doi: 10.2174/1573409915666190704093400.
- 35. MarvinSketch (21.20.0) (2021) ["Computer software"]. ChemAxon Ltd. https://chemaxon.com/products/marvin.
- 36. PyMol (2.0) (2021) ["Computer software"]. Schrödinger, LLC. https://pymol.org/2/#page-top
- 37. Aguilera Y, Estrella I, Benitez V, Esteban RM, Martín-Cabrejas MA. (2011) Bioactive phenolic compounds and functional properties of dehydrated bean flours. Food Research International, 44(3):774–780. doi: 10.1016/j.foodres.2011.01.004.
- 38. Herrera MD, Acosta-Gallegos JA, Reynoso-Camacho R, Pérez-Ramírez IF. (2019) Common bean seeds from plants subjected to severe drought, restricted- and full-irrigation regimes show differential phytochemical fingerprint. Food Chemistry, 294, 368–377. doi: 10.1016/j.foodchem.2019.05.076.
- Llorach R, Favari C, Alonso D, Garcia-Aloy M, Andres-Lacueva C, Urpi-Sarda M. (2019) Comparative metabolite fingerprinting of legumes using LC-MS-based untargeted metabolomics. Food Research International, 126, 108666. doi: 10.1016/j.foodres.2019.108666.
- Ramirez-Jimenez A, et al. (2015) 'Potential role of bioactive compounds of Phaseolus vulgaris L. on lipids-lowering mechanisms'. Food Research International. doi: 10.1016/j.foodres.2015.01.002.
- 41. Mendoza-Sánchez M, Pérez-Ramírez IF, Wall-Medrano A, Martinez-Gonzalez AI, Gallegos-Corona MA, Reynoso-Camacho R. (2019) Chemically induced common bean (*Phaseolus vulgaris* L.) sprouts ameliorate dyslipidemia by lipid intestinal absorption inhibition. Journal of Functional Foods, 52:54–62. doi: 10.1016/j.jff.2018.10.032.
- 42. Barreto NMB, Pimenta NG, Braz BF, Freire AS, Santelli RE, Oliveira AC, Bastos LHP, Cardoso MHWM, Monteiro M, Diogenes MEL, Perrone D. (2021) Organic Black Beans (*Phaseolus vulgaris* L.) from Rio de Janeiro State, Brazil, Present More Phenolic Compounds and Better Nutritional Profile Than Nonorganic. Foods, 10(4):900. doi: 10.3390/foods10040900.
- 43. Madrera RR, Valles BS. (2020) Development and



- validation of ultrasound assisted extraction (UAE) and HPLC-DAD method for determination of polyphenols in dry beans (*Phaseolus vulgaris*) Journal of Food Composition and Analysis, 85, 103334. doi: 10.1016/j.jfca.2019.103334.
- 44. García-Cordero JM, Martínez-Palma NY, Madrigal-Bujaidar E, Jiménez-Martínez C, Madrigal-Santillán E, Morales-González JA, Paniagua-Pérez R, Álvarez-González I. (2021) Phaseolin, a Protein from the Seed of Phaseolus vulgaris, Has Antioxidant, Antigenotoxic, and Chemopreventive Properties. Nutrients, 13(6): 1750. doi: 10.3390/nu13061750.
- Durango D, Quiñones W, Torres F, Rosero Y, Gil J, Echeverri F. (2002) Phytoalexin Accumulation in Colombian Bean Varieties and Aminosugars as Elicitors. Molecules, 7(11): 817–832. doi: 10.3390/71100817.
- 46. Liu Y, Ma H, Yao J. (2020) ER-α, A Key Target for Cancer Therapy: A Review. Onco Targets Ther. 2020;13:2183-2191. doi:10.2147/OTT.S236532.
- 47. Arnesen S, Blanchard Z, Williams MM, et al. (2021) ER-α Mutations in Breast Cancer Cells Cause Gene Expression Changes through Constant Activity and Secondary Effects. Cancer Res. 81(3):539-551. doi: 10.1158/0008-5472.CAN-20-1171.
- De Santo I, McCartney A, Migliaccio I, Di Leo A, Malorni L. (2019) The Emerging Role of ESR1 Mutations in Luminal Breast Cancer as a Prognostic and Predictive Biomarker of Response to Endocrine Therapy. Cancers, 11(12):1894. doi: 10.3390/cancers11121894.
- 49. Toy W, Weir H, Razavi P, Lawson M, Goeppert AU, Mazzola AM, Smith A, Wilson J, Morrow C, Wong WL, De Stanchina E, Carlson KE, Martin TS, Uddin S, Li Z, Fanning S, Katzenellenbogen JA, Greene G, Baselga J, Chandarlapaty S. (2017) Activating ESR1 Mutations Differentially Affect the Efficacy of ER Antagonists. Cancer discovery, 7(3):277–287. doi: 10.1158/2159-8290.CD-15-1523.
- 50. Puranik NV, Srivastava P, Bhatt G, John Mary DJS, Limaye AM, Sivaraman J. (2019) Determination and analysis of agonist and antagonist potential of naturally occurring flavonoids for estrogen receptor (ER- α) by various parameters and molecular modelling approach. Scientific Reports, 9(1) doi: 10.1038/s41598-019-43768-5.
- Fanning SW, Mayne CG, Dharmarajan V, Carlson KE, Martin TA, Novick SJ, Toy W, Green B, Panchamukhi S, Katzenellenbogen BS, Tajkhorshid E, Griffin PR, Shen Y, Chandarlapaty S, Katzenellenbogen JA, Greene GL. (2016) ER-α somatic mutations Y537S and D538G confer breast cancer endocrine resistance by stabilizing

- the activating function-2 binding conformation. eLife, 5, e12792. doi: 10.7554/eLife.12792.
- 52. Reva BA, Finkelstein AV, Skolnick J. (1998) What is the probability of a chance prediction of a protein structure with an rmsd of 6 å? Folding and Design, 3(2):141–147. doi: 10.1016/s1359-0278(98)00019-4.
- 53. Brzozowski AM, Pike ACW, Dauter Z, Hubbard RE, Bonn T, Engström O, ÖHman L, Greene GL, Gustafsson JK, Carlquist M. (1997) Molecular basis of agonism and antagonism in the oestrogen receptor. Nature, 389(6652):753–758. doi: 10.1038/39645.
- 54. Ye H, Shaw IC. (2019) Food flavonoid ligand structure/estrogen receptor-α affinity relationships toxicity or food functionality? Food and Chemical Toxicology, 129:328–336. doi: 10.1016/j.fct.2019.04.008.
- 55. Bitencourt-Ferreira G, de Azevedo WF. (2019) How Docking Programs Work. Methods in Molecular Biology, 35–50. doi: 10.1007/978-1-4939-9752-7 3.
- 56. Lagari VS, Levis S. (2013) Phytoestrogens in the Prevention of Postmenopausal Bone Loss. Journal of Clinical Densitometry, 16(4):445–449. doi: 10.1016/j.jocd.2013.08.011.
- 57. Tanwar AK, Dhiman N, Kumar A, Jaitak V. (2021) Engagement of phytoestrogens in breast cancer suppression: Structural classification and mechanistic approach. European Journal of Medicinal Chemistry, 213:113037. doi:10.1016/j.ejmech.2020.113037.
- 58. Manas ES, Xu ZB, Unwalla RJ, Somers WS. (2004) Understanding the Selectivity of Genistein for Human Estrogen Receptor-β Using X-Ray Crystallography and Computational Methods. Structure, 12(12):2197–2207. doi: 10.1016/j.str.2004.09.015.
- 59. Lee S, Barron MG. (2017) Structure-Based Understanding of Binding Affinity and Mode of Estrogen Receptor α Agonists and Antagonists. PloS o n e , 1 2 (1): e 0 1 6 9 6 0 7 . d o i: 10.1371/journal.pone.0169607.
- 60. D'Arrigo G, Gianquinto E, Rossetti G, Cruciani G, Lorenzetti S, Spyrakis F. (2021) Binding of Androgen- and Estrogen-Like Flavonoids to Their Cognate (Non)Nuclear Receptors: A Comparison by Computational Prediction. Molecules (Basel, Switzerland): 26(6):1613. doi: 10.3390/molecules26061613.
- 61. Chen F, Chien M. (2019) Effects of phytoestrogens on the activity and growth of primary breast cancer cells ex vivo. Journal of Obstetrics and Gynaecology Research, 45(7):1352–1362. doi: 10.1111/jog.13982.
- 62. Saarinen NM, Bingham C, Lorenzetti S, Mortensen A, Mäkelä S, Penttinen P, SØrensen IK, Valsta LM, Virgili F,



- Vollmer G, Wärri A, Zierau O. (2006) Tools to evaluate estrogenic potency of dietary phytoestrogens: A consensus paper from the EU Thematic Network "Phytohealth" (QLKI-2002-2453) Genes & Nutrition, 1(3–4):143–158. doi: 10.1007/bf02829964.
- 63. Rietjens I, Louisse J, Beekmann K. (2016) "The Potential health effects of dietary phytoestrogens". British Journal of Pharmacology 174: 1263-1280. doi:10.1111/bph.13622.
- 64. Cvejic J, Bursac M, Atanacovic M. (2012) "Phytoestrogens: "Estrogen-like" phytochemicals". Studies in Natural Products Chemistry, 38. doi: 10.1016/B978-0-444-59530-0.00001-0.
- 65. Stillwell W. (2016) An Introduction to Biological Membranes: Composition, Structure and Function. Elsevier Science.
- 66. Salehi B, Quispe C, Sharifi-Rad J, Cruz-Martins N, Nigam M, Mishra AP, Konovalov DA, Orobinskaya V, Abu-Reidah IM, Zam W, Sharopov F, Venneri T, Capasso R, Kukula-Koch W, Wawruszak A, Koch W. (2021) Phytosterols: From Preclinical Evidence to Potential Clinical Applications. Frontiers in Pharmacology, b11. doi: 10.3389/fphar.2020.599959.
- 67. Grattan BJ, Jr. (2013) Plant sterols as anticancer nutrients: evidence for their role in breast cancer. Nutrients, 5(2):359–387. doi: 10.3390/nu5020359.
- 68. Gao H, Katzenellenbogen JA, Garg R, Hansch C. (1999) Comparative QSAR Analysis of Estrogen Receptor Ligands. Chemical Reviews, 99(3):723–744. doi: 10.1021/cr980018g.
- 69. Chen M, Chen C, Shen Z, Zhang X, Chen Y, Lin F, Ma X, Zhuang C, Mao Y, Gan H, Chen P, Zong X, Wu R. (2017) Extracellular pH is a biomarker enabling detection of breast cancer and liver cancer using CEST MRI. Oncotarget, 8(28):45759–45767. doi: 10.18632/oncotarget.17404.

- 70. Sladek FM. (2011) What are nuclear receptor ligands? Molecular and cellular endocrinology, 334(1-2):3–13. doi:10.1016/j.mce.2010.06.018.
- 71. Santomasso BD. (2020) Anticancer Drugs and the Nervous System. Continuum (Minneapolis, Minn.): 26(3):732–764. doi:10.1212/CON.000000000000087.
- 72. Herman TF, Santos C. (2021) First Pass Effect. In StatPearls. StatPearls Publishing.
- 73. Levêque D, Lemachatti J, Nivoix Y, Coliat P, Santucci R, Ubeaud-Séquier G, Beretz L, Vinzio S. (2010) Mécanismes des interactions médicamenteuses d'origine pharmacocinétique. La Revue de Médecine Interne, 31(2):170–179. doi:10.1016/j.revmed.2009.07.009.
- 74. Palleria C, Di Paolo A, Giofrè C, Caglioti C, Leuzzi G, Siniscalchi A, De Sarro G, Gallelli L. (2013) Pharmacokinetic drug-drug interaction and their implication in clinical management. Journal of research in medical sciences: the official journal of Isfahan University of Medical Sciences, 18(7):601–610.
- 75. Turner A P, Alam C, Bendayan R. (2020) Efflux transporters in cancer resistance: Molecular and functional characterization of P-glycoprotein. Drug Efflux Pumps in Cancer Resistance Pathways: From Molecular Recognition and Characterization to Possible Inhibition Strategies in Chemotherapy, 1–30. doi:10.1016/b978-0-12-816434-1.00001-2.

Supplementary Table 1. *Grid Box Optimization Parameters*

Estrogen Receptors (PDB ID)	Co-crystallized ligands	x-coordinates	y-coordinates	z-coordinates	RMSD Values (Å)
1A52	E2	106.253	17.463	97.957	0.560
3UUD	E2	21.210	4.511	4.837	0.761
4ZNS	OFB	-19.390	-26.746	-6.127	0.512
4ZNV	4Q7	2.588	11.770	-20.759	0.407
5DXE	E2	25.359	-2.078	5.790	0.690
5DXG	E2	25.680	-1.720	5.847	0.866
5KCD	OB2	25.052	14.052	7.841	0.464
5KCT	OB6	-19.513	-28.461	-5.795	1.219
5KD9	OBT	-18.961	-25.460	-5.244	0.953
5TLT	7ED	18.585	12.920	3.675	1.217
5TM8	K6	-16.218	2.584	49.289	1.778
5TN4	7FZ	19.202	-1.871	2.862	0.801
5TN5	7G0	-17.011	-26.331	-2.624	1.268

Supplementary Table 2. List of secondary metabolites found in Phaseolus Vulgaris L. (fabaceae)

Count	Compounds	Aglycone	Plant Part Used	Country of Origin	Variety	References	
1	(+)-catechin glucoside	(+)-catechin	beans	Spain	Canellini and Pinta	Aguilera et al. (2011)	
2	(+)-piscidic acid	(+)-piscidic acid	pods	Spain	Perona, Helda, Strike	Abu-Reidah et al. (2012)	
3	2,6-dihydroxybenzoic acid	2,6-dihydroxybenzoic acid	beans	Mexico	Pinto Durango bean cultivar	Herrera et al. (2019)	
4	3-hydroxybenzoic acid	3-hydroxybenzoic acid	beans	Mexico	Pinto Durango bean cultivar	Herrera et al. (2019)	
5	4-hydroxybenzoic acid	4-hydroxybenzoic acid	beans	Mexico	Pinto Durango bean cultivar	Herrera et al. (2019)	
6	apigenin 6,8-di-c-glucoside	Apigenin	beans	Mexico	Pinto Durango bean cultivar	Herrera et al. (2019)	
7	aromadendrin glucoside	Aromadendrin	beans	South Africa	Mongetes del Ganxet	Llorach et al. (2019)	
8	benzoic acid	benzoic acid	beans	Mexico	Pinto Durango bean cultivar	Herrera et al. (2019)	
9	beta-sitosterol			Mexico	San Luis	Ramírez-Jiménez et al. (2015)	
10	biochanin a 7-o-[b-d-apiofuranosyl-(1>5)-b-d-apiofuranosyl-(1>6)-b-d-glucopyranoside]	Biochanin	pods	Spain	Perona, Helda, Strike	Abu-Reidah et al. (2012)	
11	caffeic acid 4-o-glucoside	caffeic acid	beans	Mexico	Pinto Durango bean cultivar	Herrera et al. (2019)	
12	β-campesterol	Campesterol	beans	Mexico	Dalia	Mendoza-Sánchez et al. (2019)	
13	carthamidin glucoside	Carthamidin	beans	South Africa	Mongetes del Ganxet	Llorach et al. (2019)	
14	chlorogenic acid	chlorogenic acid	pods	Spain	Perona, Helda, Strike	Abu-Reidah et al. (2012)	
15	chrysoeriol 7-glucoside	Chrysoreriol	pods	Spain	Perona, Helda, Strike	Abu-Reidah et al. (2012)	
16	cinnamic acid	cinnamic acid	beans	Mexico	Pinto Durango bean cultivar	Herrera et al. (2019)	
17	cis ferulic acid	cis ferulic acid	beans	Spain	Canellini and Pinta	Aguilera et al. (2011)	
18	citric acid	citric acid	beans	South Africa	Mongetes del Ganxet	Llorach et al. (2019)	

Supplementary Table 2. List of secondary metabolites found in Phaseolus vulgaris L. (Fabaceae) (continuation)

Count	Compounds	Aglycone	Plant Part Used	Country of Origin	Variety	References
19	coumesterol	Coumesterol	beans	South Africa	Mongetes del Ganxet	Llorach et al. (2019)
20	cyanidin	Cyanidin	beans	Brazil	BR1-XODÓ	Barreto et al. (2021)
21	6"-o-malonyldaidzin	Daidzein	beans	Mexico	Pinto Durango bean cultivar	Herrera et al. (2019)
22	dalbinol	Dalbinol	pods	Spain	Perona, Helda, Strike	Abu-Reidah et al. (2012)
23	dalpanin	Dalpanin	pods	Spain	Perona, Helda, Strike	Abu-Reidah et al. (2012)
24	delphinidin 3,5-o- diglucoside	Delphinidin	beans	Italy	genotype MG53	Madrera and Valles (2020)
25	delta-7-avenasterol	delta-7-avenasterol	beans	Mexico	Dalia	Mendoza-Sánchez et al. (2019)
26	eriodictyol	Eriodictyol	beans	Spain	Canellini and Pinta	Aguilera et al. (2011)
27	escopoletin	Escopoletin	beans	Spain	Canellini and Pinta	Aguilera et al. (2011)
28	hydroxybenzyl-malic acid (eucomic acid)	eucomic acid	beans	South Africa	Mongetes del Ganxet	Llorach et al. (2019)
29	formononetin 7-o-glucoside (ononin)	Formononetin	pods	Spain	Perona, Helda, Strike	Abu-Reidah et al. (2012)
30	fucosterol	Fucosterol	beans	Mexico	Dalia	Mendoza-Sánchez et al. (2019)
31	gallic acid 4-o-glucoside	gallic acid	beans	Mexico	Pinto Durango bean cultivar	Herrera et al. (2019)
32	gallic acid ethyl ester	gallic acid ethyl ester	beans	Mexico	Pinto Durango bean cultivar	Herrera et al. (2019)
33	6"-o-malonylgenistin	Genistein	beans	Mexico	Pinto Durango bean cultivar	Herrera et al. (2019)
34	genistin	Genistin	beans	Mexico	Pinto Durango bean cultivar	Herrera et al. (2019)
35	gibberellin a 19	gibberellin a 19	beans	South Africa	Mongetes del Ganxet	Llorach et al. (2019)
36	gibberellin a25	gibberellin a25	beans	South Africa	Mongetes del Ganxet	Llorach et al. (2019)
37	gibberellin a38	gibberellin a38	beans	South Africa	Mongetes del Ganxet	Llorach et al. (2019)
38	6"-o-malonylglycitin	Glycitein	beans	Mexico	Pinto Durango bean cultivar	Herrera et al. (2019)
39	heliangin	Heliangin	beans	South Africa	Mongetes del Ganxet	Llorach et al. (2019)
40	hesperidin	Hesperitin	beans	Mexico	Dalia	Mendoza-Sánchez et al. (2019)
41	hydroxyeucomic acid	hydroxyeucomic acid	beans	South Africa	Mongetes del Ganxet	Llorach et al. (2019)
42	hydroxymethoxycinnamic acid	hydroxymethoxycinnamic acid	beans	South Africa	Mongetes del Ganxet	Llorach et al. (2019)
43	isoferulic acid	isoferulic acid	beans	Mexico	Pinto Durango bean cultivar	Herrera et al. (2019)
44	isolariciresinol 9-o-b-d - glucopyranoside i	Isolariciresinol	pods	Spain	Perona, Helda, Strike	Abu-Reidah et al. (2012)
45	isorhamnetin 3-glucuronide	Isorhamnetin	pods	Spain	Perona, Helda, Strike	Abu-Reidah et al. (2012)
46	isosakuranetin 7-rutinoside	Isosakuranetin	pods	Spain	Perona, Helda, Strike	Abu-Reidah et al. (2012)
47	kaempferol-rutinoside	Kaempferol	beans	South Africa	Mongetes del Ganxet	Llorach et al. (2019)
48	kutkoside	kutkoside aglycone	pods	Spain	Perona, Helda, Strike	Abu-Reidah et al. (2012)
49	luteolin 7-o-rutinoside	Luteolin	beans	Mexico	Pinto Durango bean cultivar	Herrera et al. (2019)
50	malvidin 3-glucoside	Malvidin	beans	Brazil	BR1-XODÓ	Barreto et al. (2021)
51	myricetin	Myricetin	beans	Italy	genotype MG76	Madrera and Valles (2020)

Supplementary Table 2. List of secondary metabolites found in Phaseolus vulgaris L. (Fabaceae) (continuation)

Count	Compounds	Aglycone	Plant Part Used	Country of Origin	Variety	References
52	naringenin	Naringenin	beans	Spain	Canellini and Pinta	Aguilera et al. (2011)
53	naringenin 7-methyl ether	naringenin 7-methyl ether	beans	Spain	Canellini and Pinta	Aguilera et al. (2011)
54	naringin	Naringin	beans	Mexico	Pinto Durango bean cultivar	Herrera et al. (2019)
55	pelargonidin	Pelargonidin	beans	Brazil	BR1-XODÓ	Barreto et al. (2021)
56	peonidin	Peonidin	beans	Brazil	BR1-XODÓ	Barreto et al. (2021)
57	petunidin 3,5-o-diglucoside	Petunidin	beans	Italy	genotype MG55	Madrera and Valles (2020)
58	phaseolin	Phaseolin	beans	Mexico		García-Cordero et al. (2021)
59	phaseollinisoflavan	Phaseollinisoflavan	beans	Colombia	Cargamanto Blanco and ICA Quimbaya	Durango et al. (2002)
60	p-hydroxyphenyl acetic acid	p-hydroxyphenyl acetic acid	beans	Spain	Canellini and Pinta	Aguilera et al. (2011)
61	pinocembrin	Pinocembrin	beans	Spain	Canellini and Pinta	Aguilera et al. (2011)
62	procyanidin dimer b1	procyanidin dimer b1	beans	Mexico	Pinto Durango bean cultivar	Herrera et al. (2019)
63	procyanidin dimer b2	procyanidin dimer b2	beans	Mexico	Pinto Durango bean cultivar	Herrera et al. (2019)
64	procyanidin trimer c1	procyanidin trimer c1	beans	Mexico	Pinto Durango bean cultivar	Herrera et al. (2019)
65	procyanidin trimer c2	procyanidin trimer c2	beans	Mexico	Pinto Durango bean cultivar	Herrera et al. (2019)
66	prodelphinidin b	prodelphinidin b	beans	South Africa	Mongetes del Ganxet	Llorach et al. (2019)
67	protocatechuic acid 4-o- glucoside	protocatechuic acid	beans	Mexico	Pinto Durango bean cultivar	Herrera et al. (2019)
68	isoquercitrin	Quercetin	beans	South Africa	Mongetes del Ganxet	Llorach et al. (2019)
69	resveratrol glucoside	Resveratrol	beans	South Africa	Mongetes del Ganxet	Llorach et al. (2019)
70	rhamnetin	Rhamnetin	beans	Mexico	Pinto Durango bean cultivar	Herrera et al. (2019)
71	salicylic acid	salicylic acid	beans	Spain	Canellini and Pinta	Aguilera et al. (2011)
72	sinapic acid	sinapic acid	beans	Italy	genotype MG52	Madrera and Valles (2020)
73	soyasapogenol a	soyasapogenol A	beans	Mexico	Pinto Durango bean cultivar	Herrera et al. (2019)
74	soysaponin αg	oyasapogenol B	beans	Mexico	Dalia	Mendoza-Sánchez et al. (2019)
75	soyasapogenol d	soyasapogenol D	beans	Mexico	Pinto Durango bean cultivar	Herrera et al. (2019)
76	soyasapogenol e	soyasapogenol E	beans	Mexico	Pinto Durango bean cultivar	Herrera et al. (2019)
77	phaseoside i	soyaspogenol A	beans	Mexico	Dalia	Mendoza-Sánchez et al.
78	stigmasterol	Stigmasterol	beans	Mexico	San Luis	Ramírez-Jiménez et al. (2015)
79	taxifolin 3-o-rhamnoside	Taxifolin	pods	Spain	Perona, Helda, Strike	Abu-Reidah et al. (2012)
80	trans p-coumaroyl aldaric acid	trans p-coumaric acid	beans	Spain	Canellini and Pinta	Aguilera et al. (2011)
81	trans ferulic acid	trans ferulic acid	beans	Spain	Canellini and Pinta	Aguilera et al. (2011)
82	tryptophol	Tryptophol	beans	Spain	Canellini and Pinta	Aguilera et al. (2011)
83	vanillic acid b-glucoside	vanillic acid	pods	Spain	Perona, Helda, Strike	Abu-Reidah et al. (2012)

Supplementary Table 3. Compounds from Phaseolus vulgaris L. (Fabaceae) which exhibited favorable oral bioavailability, human intestinal absorption, drug-likeness, and toxicity

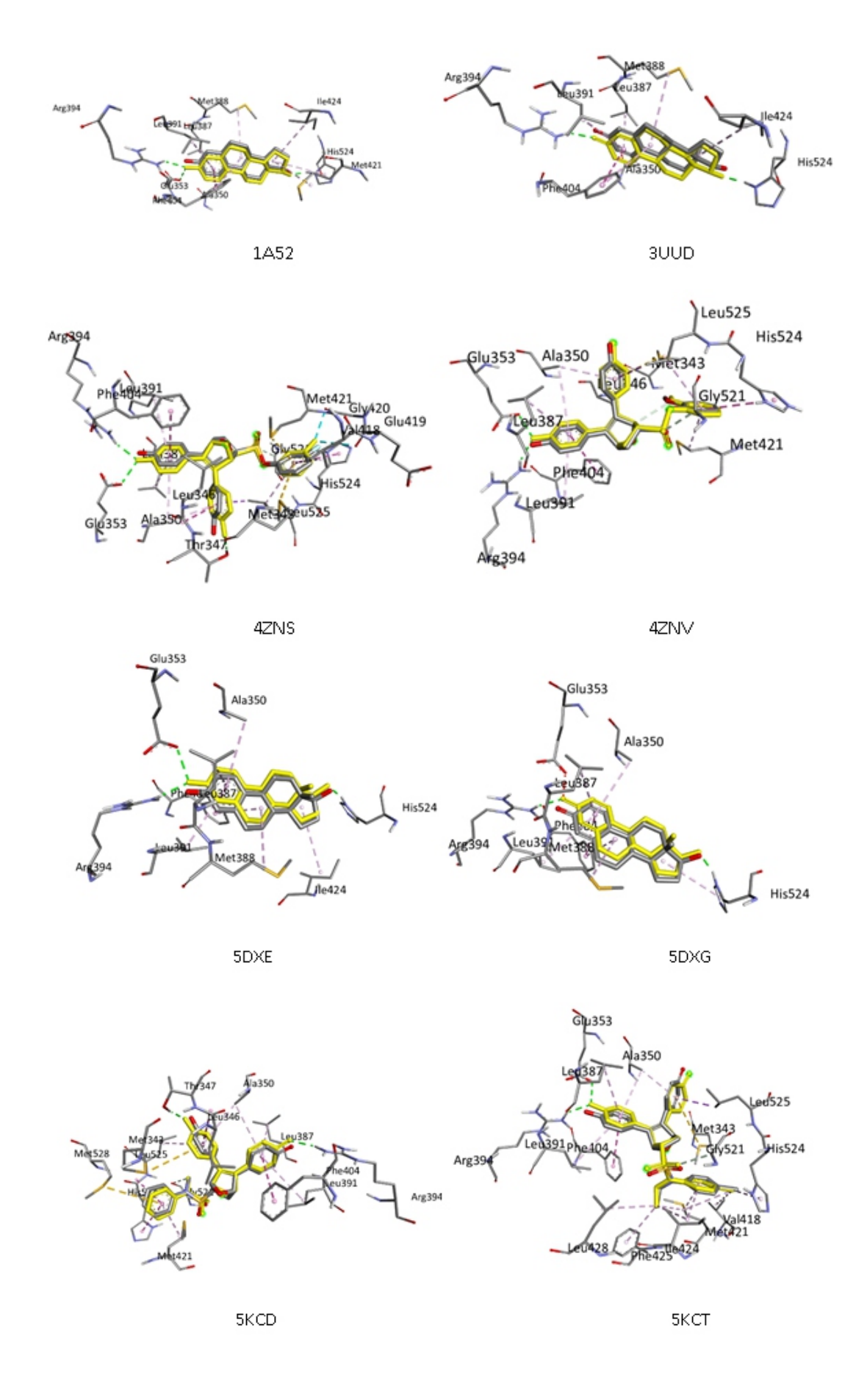
Count	Compounds	HIA	F(20%)	F(30%)	Carcinogenicity	Non Genotoxic ^⁵ Carcinogenicity	Genotoxic/ Carcinogenicity/ Mutagenicity	QED	Lipinski	ERA ^c as target
1	(+)-catechin ^A	0.035	0.998	1	0.185	0	0	0.51	Accepted	NP
2	(+)-piscidic acid ^A	0.132	0.042	0.089	0.007	0	0	0.465	Accepted	Y
3	2,6-dihydroxybenzoic acid	0.079	0.579	0.993	0.152	0	0	0.559	Accepted	N
4	3-hydroxybenzoic acid	0.01	0.017	0.571	0.026	0	0	0.61	Accepted	N
5	3-hydroxybenzoic acid	0.01	0.01	0.308	0.05	0	0	0.61	Accepted	N
6	apigenin	0.015	0.995	0.999	0.277	0	0	0.632	Accepted	Y
7	aromadendrin ^A	0.012	0.715	0.099	0.039	0	0	0.634	Accepted	NP
8	benzoic acid	0.013	0.003	0.011	0.026	0	0	0.611	Accepted	N
9	beta-sitosterol ^A	0.002	0.889	0.054	0.12	0	0	0.436	Accepted	Y
10	biochanin ^A	0.005	0.008	0.795	0.221	0	0	0.756	Accepted	N
11	campesterol ^A	0.002	0.942	0.059	0.148	0	0	0.47	Accepted	Y
12	Carthamidin	0.031	0.957	0.996	0.581	0	0	0.599	Accepted	Y
13	Chrysoeriol	0.032	0.95	0.998	0.083	0	0	0.672	Accepted	Y
14	citric acid	0.398	0.008	0.004	0.009	0	0	0.427	Accepted	N
15	Cyanidin	0.028	0.997	0.998	0.069	0	0	0.347	Accepted	N
16	Daidzein	0.008	0.23	0.856	0.617	0	0	0.7	Accepted	Y
17	Dalpanin	0.01	0.786	0.838	0.169	0	0	0.639	Accepted	N
18	delphinidin	0.054	0.999	0.999	0.04	0	0	0.301	Accepted	N
19	delta_7_avenasterol ^A	0.005	0.99	0.857	0.008	0	0	0.454	Accepted	Y
20	eriodictyol ^A	0.01	0.794	0.999	0.509	0	0	0.599	Accepted	Υ
21	formononetin	0.004	0.006	0.896	0.488	0	0	0.775	Accepted	Y
22	fucosterol ^A	0.003	0.987	0.253	0.157	0	0	0.454	Accepted	Y
23	gallic acid	0.085	0.964	0.995	0.024	0	0	0.46	Accepted	N
24	gallic acid ethyl ester	0.013	0.794	0.961	0.035	0	0	0.487	Accepted	N
25	Genistein	0.01	0.863	0.992	0.316	0	0	0.632	Accepted	Y
26	gibberellin A19 ^A	0.016	0.611	0.048	0.376	0	0	0.524	Accepted	N
27	gibberellin A25 ^A	0.023	0.947	0.038	0.148	0	0	0.665	Accepted	N
28	gibberellin A38 ^A	0.014	0.943	0.265	0.881	0	0	0.482	Accepted	N
29	glycitein	0.005	0.008	0.199	0.393	0	0	0.756	Accepted	N
30	hesperitin ^A	0.007	0.009	0.974	0.522	0	0	0.789	Accepted	Y
31	isolariciresinol ^A	0.054	0.203	0.012	0.06	0	0	0.651	Accepted	Y
32	Isorhamnetin	0.024	0.03	0.978	0.047	0	0	0.572	Accepted	N
33	isosakuranetin ^A	0.005	0.003	0.905	0.674	0	0	0.887	Accepted	Y
34	Kaempferol	0.008	0.856	0.993	0.097	0	0	0.546	Accepted	Y
35	luteolin	0.047	0.998	1	0.095	0	0	0.511	Accepted	Y
36	malvidin	0.038	0.046	0.731	0.032	0	0	0.545	Accepted	N

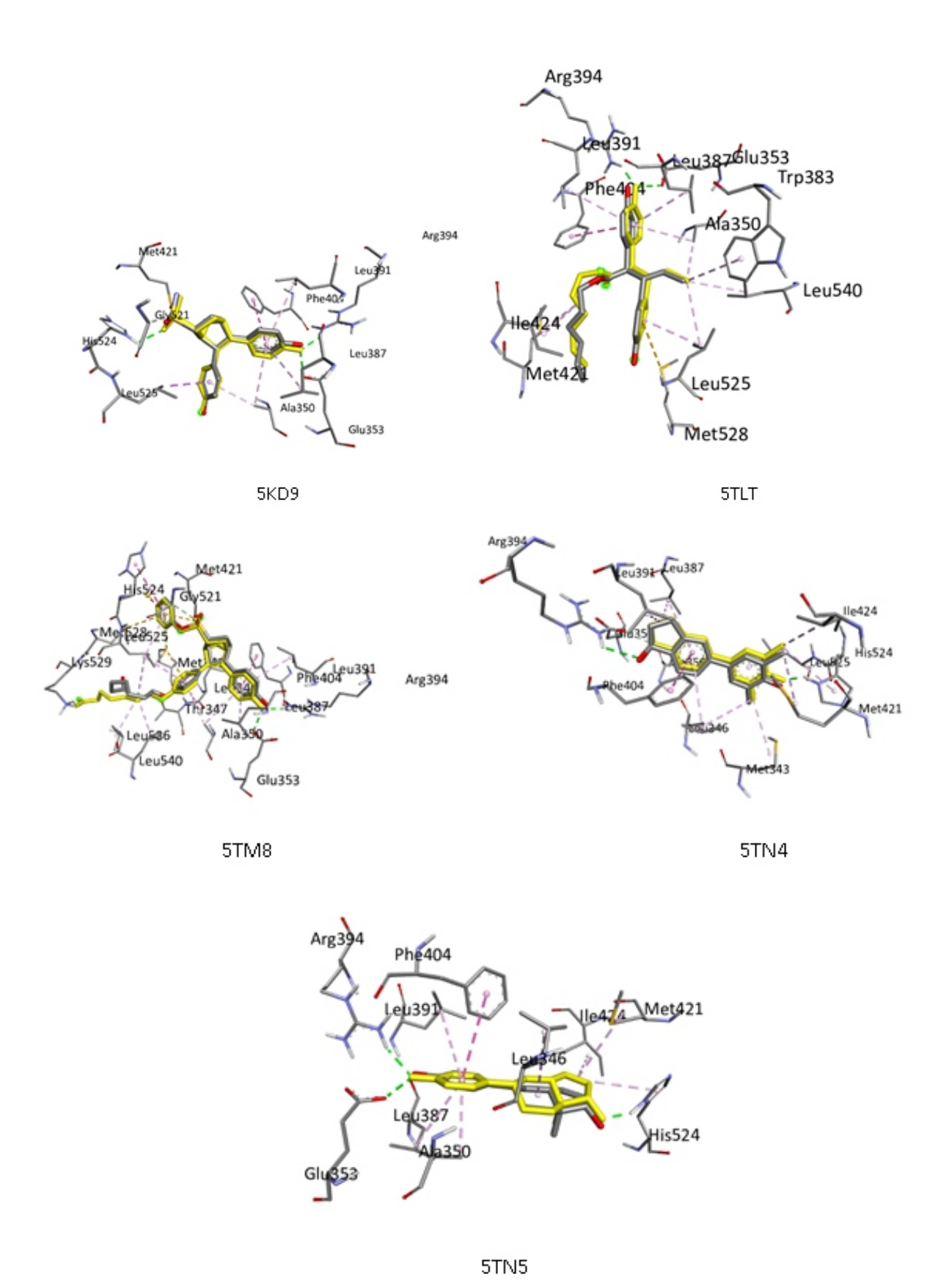
Supplementary Table 3. Compounds from Phaseolus vulgaris L. (Fabaceae) which exhibited favorable oral bioavailability, human intestinal absorption, drug-likeness, and toxicity (continuation)

Count	Compounds	HIA	F(20%)	F(30%)	Carcinogenicity	Non Genotoxic ^в Carcinogenicity	Genotoxic/ Carcinogenicity/ Mutagenicity	QED	Lipinski	ERA ^c as target
37	methyl 2-hydroxy-4- methoxy-6- methylbenzoate	0.012	0.006	0.274	0.032	0	0	0.728	Accepted	N
38	myricetin	0.035	0.977	0.999	0.028	0	0	0.371	Accepted	N
39	naringenin	0.018	0.972	0.997	0.576	0	0	0.742	Accepted	Y
40	naringenin 7-methyl ether ^A	0.005	0.003	0.857	0.685	0	0	0.887	Accepted	Y
41	pelargonidin	0.014	0.991	0.996	0.13	0	0	0.51	Accepted	Υ
42	peonidin	0.012	0.951	0.984	0.073	0	0	0.542	Accepted	Υ
43	petunidin	0.03	0.981	0.994	0.036	0	0	0.364	Accepted	Υ
44	phaseollinisoflavan ^A	0.01	0.005	0.004	0.861	0	0	0.832	Accepted	Υ
45	phaseolin ^A	0.015	0.002	0.003	0.719	0	0	0.79	Accepted	Υ
46	p-hydroxyphenyl acetic acid	0.013	0.024	0.007	0.382	0	0	0.665	Accepted	Y
47	pinocembrin ^A	0.006	0.035	0.992	0.654	0	0	0.823	Accepted	Υ
48	protocatechuic acid	0.032	0.367	0.97	0.046	0	0	0.522	Accepted	N
49	Quercetin	0.014	0.93	0.997	0.05	0	0	0.434	Accepted	N
50	Resveratrol	0.012	0.264	0.055	0.287	0	0	0.692	Accepted	Υ
51	Rhamnetin	0.02	0.011	0.98	0.058	0	0	0.535	Accepted	N
52	salicylic acid	0.017	0.008	0.838	0.046	0	0	0.61	Accepted	N
53	sandosaponin aglycone	0.03	0.125	0.846	0.08	0	0	0.454	Accepted	Υ
54	soyasapogenol A ^A	0.006	0.893	0.726	0.121	0	0	0.399	Accepted	Υ
55	soyasapogenol B ^A	0.006	0.525	0.617	0.058	0	0	0.415	Accepted	Υ
56	soyasapogenol D ^A	0.009	0.9	0.947	0.014	0	0	0.429	Accepted	Υ
57	soyasapogenol E ^A	0.011	0.909	0.968	0.222	0	0	0.454	Accepted	Y
58	stigmasterol ^A	0.009	0.992	0.552	0.1	0	0	0.457	Accepted	Υ
59	Taxifolin	0.014	0.892	0.678	0.039	0	0	0.501	Accepted	NP
60	Trytophol	0.013	0.716	0.987	0.151	0	0	0.691	Accepted	N
61	vanillic acid	0.013	0.01	0.655	0.062	0	0	0.693	Accepted	N

^Aisomeric SMILES strings were used in the ADMETlab2.0 web server as input ^BPresence (1) or Absence (0) of toxicophore leading to cancer via nongenotoxic mechanisms

^cERA stands for ER-α and these results were obtained from Swiss Target Prediction webserver (http://www.swisstargetprediction.ch/); NP= no similar actives predicted in the database; Y= Yes; N= No





Supplementary Figure 1. Superimposed images of the original and redocked poses of the co-crystallized ligands to its corresponding receptor. Shown in yellow is the original pose of the co-crystallized ligand whereas the redocked poses are shown in gray.